Convergent evolution on oceanic islands: comparative genomics reveals species-specific processes in birds

María Recuerda

  Cornell Lab of Ornithology, Cornell University

Julio César Hernández Montoya

  Grupo de Ecología y Conservación de Islas, A. C.

Guillermo Blanco

  Museo Nacional de Ciencias Naturales (MNCN), CSIC.

Borja Milá

  `b.mila@csic.es`

  Museo Nacional de Ciencias Naturales (MNCN), CSIC.

Research Article

Additional Declarations: No competing interests reported.

1 **Convergent evolution on oceanic islands: comparative genomics reveals species-specific processes in**

2 **birds**

3

4 María Recuerda [1,2], Julio César Hernández Montoya [3], Guillermo Blanco [1], Borja Milá [1]

5 [1] Museo Nacional de Ciencias Naturales (MNCN), CSIC, Calle José Gutiérrez Abascal 2, Madrid 28006,

6 Spain.

7 [2] Cornell Laboratory of Ornithology, Cornell University, Ithaca, NY, USA

8 [3] Grupo de Ecología y Conservación de Islas, A. C., Ensenada, Baja California, México

9
10

11

12 Corresponding authors: María Recuerda, Cornell Laboratory of Ornithology, Cornell University, Ithaca,

13 NY, USA, Email: mariarecuerdacarrasco@gmail.com; and Borja Milá, Museo Nacional de Ciencias

14 Naturales, Calle José Gutiérrez Abascal 2, Madrid 28006, Spain; Tel. +34 914111328, Email:

15 b.mila@csic.es

16

17

18 ORCID numbers:
19 María Recuerda: 0000-0001-9647-3627
20 Julio César Hernández Montoya: 0000-0001-9703-8491
21 Guillermo Blanco: 0000-0001-5742-4929
22 Borja Milá: 0000-0002-6446-0079
23 Declarations of interest: none

24   **Abstract**

25   Understanding the factors driving phenotypic and genomic differentiation of insular populations is of

26   major interest to gain insight into the speciation process. Comparing patterns across different insular

27   taxa subjected to similar selective pressures upon colonizing oceanic islands provides the opportunity to

28   study parallel evolution and identify shared patterns in their genomic landscapes of differentiation. We

29   selected four species of passerine birds (common chaffinch *Fringilla coelebs/canariensis*, red-billed

30   chough *Pyrrhocorax pyrrhocorax, house finch Haemorhous mexicanus* and dark-eyed/island junco *Junco*

31   *hyemalis/insularis)* that have both mainland and insular populations. For each species, we sequenced

32   whole genomes from mainland and insular individuals to infer their demographic history, characterize

33   their genomic differentiation, and identify the factors shaping them. We estimated the relative (F_{ST}) and

34   absolute (d_{xy}) differentiation, nucleotide diversity (π), Tajima's D, gene density and recombination rate.

35   We also searched for selective sweeps and chromosomal inversions along the genome. Changes in body

36   size between island and mainland were consistent with the island rule. All species shared a marked

37   reduction in effective population size (N_e) upon island colonization. We found highly differentiated

38   genomic regions in all four species, suggesting the role of selection in island-mainland differentiation,

39   yet the lack of congruence in the location of these regions indicates that each species adapted to insular

40   environments differently. Our results suggest that the genomic mechanisms involved, which include

41   selective sweeps, chromosomal inversions, and historical factors like recurrent selection, differ in each

42   species despite the highly conserved structure of avian genomes and the similar selective factors

43   involved.

44

45

46   **Keywords:** Comparative genomics, island rule, parallel evolution, speciation.

Introduction

The colonization of oceanic islands by mainland individuals has been a major engine of biological diversification, resulting in the evolution of thousands of new species across the world (1–5). These colonization events have also provided valuable research models to study processes like evolutionary divergence and local adaptation (6–8). Upon colonization of oceanic islands, individuals across taxonomic groups have often been subjected to similar demographic and selective factors, like population bottlenecks, strong selection for local adaptation, and reduced dispersal (9,10). Shared patterns of phenotypic evolution of insular populations across taxonomic groups has led to general biogeographic rules, like Foster's rule, also known as the "island rule", which postulates that on islands small animals tend to become larger, and large animals tend to become smaller (11–13). These patterns suggest the possibility of parallel evolution across species, and provide the opportunity to test whether the selective mechanisms acting during island colonization are shared across species, and whether selection acts on the same or different genomic loci.

The genomic underpinnings of divergence in oceanic islands are poorly understood, yet an increasing number of studies are addressing this topic thanks to the recent advances in high-throughput DNA sequencing (reviewed in (14). Both selection and drift can drive phenotypic changes in islands, yet patterns of parallel phenotypic change are more likely to be driven by selection than by random drift (15,16). Parallel phenotypic changes on islands could be promoted by similar selective pressures due to their particular features relative to the mainland, such as simplified ecosystems, reduced trophic resources, the availability of new ecological niches, a reduction in predation which often leads to an increase in intraspecific competition, and a reduction in interspecific competition (7,17). These insular selective pressures usually result in predictable changes in body size (13), usually attributed to the absence of predators and the shifts in competition, and also result in diet shifts in order to adapt to the new trophic resources, leading to behavioral (18,19), morphological (20,21) and physiological adaptations (22,23). The molecular basis of convergent phenotypic traits across species could be entirely species-specific, or instead show evolutionary convergence among species. The degree of molecular parallelism can range from sharing the same mutation on the same gene, to changes at different nucleotides within the same gene, to changes in different genes within the same pathway (14,24). The probability of molecular parallelism is determined by several factors, increasing when selective pressures are similar and genomic constraints such as demography and phylogenetic history are shared (16). The genetic basis of the phenotypic traits under selection is also important: single-locus traits have

79 been often involved in repeated convergent evolution (e.g., (25,26), yet for polygenic traits, which can

80 be modified through multiple pathways, molecular parallelism becomes less likely (16,27,28) resulting

81 instead in heterogeneous, species-specific patterns of differentiation.

82

83 Understanding the factors that generate heterogeneous patterns of differentiation across the genome is

84 one of the main goals of population genomics (29–33). The main factors shaping differentiation patterns

85 are drift and selection, but demographic history and genomic features such as recombination rate and

86 gene content also affect the distribution of the differentiated regions (31). Recent advances in

87 sequencing technologies have allowed studying the genomic landscapes of variation, which show the

88 distributional pattern of genomic variation across the entire genome (34–37). When comparing

89 differentiated populations, regions that are highly divergent relative to the genomic background are

90 known as "islands of differentiation" (34,38) and are usually detected as regions of high relative

91 divergence (F_{ST}, (39). Early genome scans interpreted F_{ST} peaks as signatures of strong selection

92 surrounded by valleys homogenized by gene flow (40), where those F_{ST} peaks were caused by marked

93 differences in allele frequencies at locally adapted sites and the neutral loci linked to them (41,42).

94 However, when considering patterns of absolute divergence (d_{xy}) and within-population diversity (π)

95 besides F_{ST}, new interpretations of how these islands of differentiation originate have been put forward.

96 F_{ST} peaks could also appear when population diversity is low in either of the populations compared,

97 while d_{xy} is less affected by this pattern. Several processes such as positive and/or background selection

98 can reduce within population nucleotide diversity and generate "islands" of relative divergence, while

99 absolute divergence remains unchanged (29,43,44). Four models have been proposed to explain the

100 underlying cause of islands of differentiation (Irwin et al., 2016; Irwin et al., 2018) and in order to

101 differentiate these models it is crucial to understand the relationship between F_{ST}, d_{xy} and π (29,44–46).

102 Two of those models account for speciation in the presence of gene flow ("divergence-with-gene-flow"

103 and "sweep-before-differentiation") and the other two involve allopatric speciation ("Selection in

104 allopatry" and "Recurrent selection") (45). Moreover, other factors such as demographic history,

105 mutation rate heterogeneity, and recombination rate across the genome, as well as gene density, could

106 modify the genomic landscape (31). Therefore, to correctly interpret the genomic landscapes of

107 differentiation it is important to understand the demographic and evolutionary history of the target taxa

108 (31). Variations in effective population size (N_e) can produce different genomic signatures. For instance,

109 marked reductions in N_e such as those caused by population bottlenecks at founder events, can modify

110 levels of background selection and therefore the baseline for the detection of outlier loci (47,48).

111

112   Covariation of genomic patterns of differentiation among different avian species has been shown across

113   broad evolutionary timescales (49–52) and the coincident location of differentiation peaks has been of

114   special interest to understand the process of convergent molecular evolution where similar loci evolve

115   independently in several species (53). Bird genomes show high synteny (54), a relatively stable number

116   of chromosomes (55), similar recombination landscapes (56,57), and across species microchromosomes

117   show higher density in gene content than macrochromosomes (56,58). The similarity in genomic

118   landscapes of differentiation across closely related and diverged avian species could be due to the non-

119   random distribution of gene content across the genome and the coincidence of low recombination areas

120   along with linked selection (44,49), since it has been shown that the recombination landscape in birds

121   can be maintained across species over long evolutionary time periods (56).

122

123   Here we use a comparative approach to examine patterns of genome-wide differentiation in avian

124   species that have colonized oceanic islands, with the goal of assessing the relative roles of demographic

125   history, time of divergence, and directional selection in driving divergence and potentially evolutionary

126   convergence upon island colonization. We selected four passerine species that have mainland

127   populations and have also colonized oceanic islands; two species from mainland Europe that have

128   colonized the island of La Palma in the Canary Islands, Atlantic Ocean, the common chaffinch (*Fringilla*

129   *coelebs/canariensis*) and the red-billed chough (*Pyrrhocorax pyrrhocorax*), and two species from North

130   America that have colonized Guadalupe Island on the Pacific Ocean, the house finch (*Haemorhous*

131   *mexicanus*) and the dark-eyed junco (*Junco hyemalis/insularis*). The red-billed chough and the house

132   finch have diverged from mainland populations within the last 100,000 years, whereas the common

133   chaffinch and the junco have been separated from their mainland relatives for over 500,000 years (59–

134   61). Given that all four species have colonized oceanic islands and have been subjected to potentially

135   similar selective pressures, we first analyzed if the differences phenotype between insular and mainland

136   counterparts affected the same traits across species. Changes in morphological traits are expected upon

137   colonization of the new insular environment (4,10) and those changes are likely to generate detectable

138   genomic signatures. Therefore, we also asked if the genomic landscapes of differentiation are similar

139   among species when taking divergence time into account.

140

141   We performed whole-genome resequencing of 9-12 individuals per treatment per species in order to

142   determine whether the four species showed similar patterns of differentiation in their genomic

143   landscapes, and whether these patterns have been shaped by similar processes. We studied the

144   demographic history and performed genomic scans of F_{ST}, d_{xy}, π, Tajima's D, recombination rate, gene

145   content and selective sweeps. We also scanned the genomes looking for putative chromosomal

146   inversions, which have been shown to underlie major phenotypic polymorphisms in birds (62). We

147   detected regions under selection among insular and mainland counterparts as F_{ST} outliers and selective

148   sweeps, and identified shared candidate genes among the four species. Comparing the genomic

149   signatures of island colonization in four different species that have been exposed to similar selective

150   pressures and that differ in colonization time (which can be considered as a proxy for different stages

151   along the speciation continuum), can provide useful understanding for the mechanisms shaping the

152   genomic landscapes through the divergence process over time.

153

154   **Methods**

155   ***Study Area and fieldwork***

156   We sampled mainland populations of the common chaffinch (Fringillidae: *Fringilla coelebs*) and the red-

157   billed chough (Corvidae: *Pyrrhocorax pyrrhocorax*) in the Iberian Peninsula at Segovia and Los Monegros,

158   respectively (see (60,61). The insular populations from both species were sampled in La Palma, the most

159   north-western island of the Canary Islands archipelago (Fig. 1A, Table S1). The common chaffinch lineage

160   in the Canary Islands has recently been raised to species status (63), and we use its current name,

161   Canary Islands chaffinch (*Fringilla canariensis*). The mainland populations of the house finch (Fringillidae:

162   *Haemorhous mexicanus*) and dark-eyed junco (Passerellidae: *Junco hyemalis oreganus*) were sampled in

163   California, and two house finch individuals were sampled in Sierra Juarez (Baja California, Mexico).

164   Insular populations for both species were sampled in Guadalupe Island, Mexico, in the Pacific Ocean

165   (Fig. 1B, Table S1). The junco on Guadalupe Island, until recently a subspecies of *J. hyemalis*, has been

166   raised to species status, and we use its current name, island junco (*Junco insularis*).

167

168   All individuals were captured in the field using mist nets, and also mesh traps in the case of red-billed

169   choughs. All individuals were marked with uniquely numbered aluminum bands, sexed, aged and

170   measured. A blood sample was obtained by venipuncture of the sub-brachial vein and stored in absolute

171   ethanol at -20°C in the laboratory for DNA extraction. After processing, birds were released unharmed at

172   the site of capture. We determined the sex of choughs by the amplification of the *Chd1* gene following

173   Griffiths et al. (64).

174

Morphological data and analysis

176

177 We compared the morphological traits of adult males from mainland and insular populations for all

178 species using principal components analysis (PCA) of all variables and univariate analysis of variance

179 (ANOVA) to compare the means among treatments for each species. For the common chaffinch, the

180 junco and the house finch a wing ruler was used to measure unflattened wing length to the nearest 0.5

181 mm, and dial callipers of 0.1-mm precision were used to measure tail length, tarsus length, bill culmen,

182 total bill length, bill width and bill depth, following Milá et al.(65). All measurements were taken by a

183 single observer (BM). For the red billed chough, the same traits were measured by a single observer (GB)

184 following standard methods described previously (66).

185 The PCA including all morphological variables was computed using the _prcomp_ function in _stats_ R

186 package.

Genome resequencing

188 Genomic DNA was extracted with a QIAGEN Blood and Tissue kit following the manufacturer's protocol.

189 Resequencing at 18x coverage of 24 individuals per species (12 per treatment, but only 9 for the

190 mainland common chaffinch) was conducted on a SE50 Illumina™ platform at Novogene™. Reads were

191 trimmed with _Trim Galore_ (67) and mapped to their respective reference genomes using BWA (Burrows-

192 Wheeler Aligner, (68). For the common chaffinch and the house finch we used the common chaffinch

193 reference genome (GCA_015532645.2, (69); for the junco we used the _Junco hyemalis_ reference

194 genome (GCA_003829775.1, (70); and for the red-billed chough we used the _Corvus moneduloides_

195 reference genome (GCA_009650955.1, bCorMon1.pri). SNPs were called using BCFTOOLS v.1.3.1 (71)

196 including invariant sites. Filtering was performed with VCFTOOLS v. 0.1.15 (72) separately for variant and

197 invariant sites, using the following criteria for variant sites: (i) Indels and sites with more than two alleles

198 were removed; (ii) a number of reads per site between 10 and 40; (iii) a minimal genotype quality of 30;

199 (iv) a minor allele frequency of 0.01; and (v) 25% maximum missing data and for invariant sites a

200 minimal genotype quality of 30. Variant and invariant sites were then merged using BCFTOOLS concat.

201 The reference genomes from all four species were aligned to the zebra finch genome (_Taeniopygia_

202 _guttata_**,** bTaeGut2.pat.W.v2) using nucmer from the MUMmer package (v.4.0, '-b 400' and filtering with

203 'delta-filter -1'; (73) and chromosomes were numbered accordingly (see Table S2, Fig. S1).

204

205 *Inference of demographic history*

206 The change in effective population size (N_e) across time for each species was estimated using Pairwise

207 Sequentially Markovian Coalescent (PSMC) analysis (74). The PSMC model infers demographic history

208 based on genome-wide heterozygous sequence data. We used SAMTOOLS (75) to obtain diploid

209 consensus sequences from BAM files generated with BWA-mem (68). Sites with sequencing depth lower

210 than 10 and higher than 35 were removed. Because sex chromosomes can show different rates and

211 patterns of evolution than autosomes (reviewed by (44,76), we focused our comparisons of

212 differentiation statistics on autosomes only. We converted the diploid consensus sequence to PSMC

213 input files (psmcfa) using the tool fq2psmcfa included in the PSMC software. Then, the program PSMC

214 was used to infer the population history with the options '-N25 –t5 –r1 –p "4+30*2+4+6+10', except for

215 the mainland common chaffinch, and for both populations of the house finch, where the upper time

216 limit was set to 1 (-t1) to achieve convergence. We performed 100 bootstraps for one genome per

217 species and treatment. The atomic time interval was set following Nadachowska-Brzyska et al., (77). We

218 used a mutation rate of 4.6 e-9 mutations/site/generation (78), which has been used in other avian

219 systems for PSMC analysis (e.g., (21,79–81). Generation time was set to two years for all species (82–

220 84).

221

222 *Inference of recombination rate*

223 In order to determine the effect of recombination rate on the genomic landscapes of differentiation, we

224 estimated recombination rates across the genome for insular and continental populations for the four

225 species using LDhat software (85). First, we created a modified likelihood lookup table based on the

226 LDhat precomputed tables using a sample size of 12 per treatment (9 for the continental common

227 chaffinch) and a population mutation rate parameter estimate of 0.001. Then vcf files were split into

228 chunks of 10,000 SNPs and converted to ldhat format using VCFTOOLS v. 0.1.15 (72). The input files

229 generated were used in LDhat "interval" to estimate the effective recombination rate by implementing a

230 Bayesian MCMC sampling algorithm with five million iterations, sampling every 5,000 steps and a block

231 penalty of 10. Finally, the results were summarized using the LDhat module "stat", discarding 20% of the

232 samples as burn-in.

233

234   ***Genome scans and detection of selective sweeps***

235   In order to detect genomic signatures of selection among the island and mainland counterparts from the

236   four different species, we estimated two different statistics, the fixation index (F_{ST}, (39) and the cross-

237   population extended haplotype homozygosity (XP-EHH) (86). First, F_{ST}, d_{xy} and π using were calculated in

238   non-overlapping windows of 10Kb using pixy v. 2 (87). Pixy takes into account the invariant sites for π

239   and d_{xy} calculations, thus overcoming the problem of most programs that use VCF files to calculate those

240   statistics but do not distinguish among invariant and missing sites, resulting in deflated estimates (87).

241   We also computed Tajima's D (72,88) in non-overlapping 10-Kb windows with VCFTOOLS (72,89). The

242   averaged values of each variable were then transformed to Z-scores using the "scale" command in R. To

243   detect F_{ST}, outliers we corrected for multiple testing setting the false discovery rate (FDR) to 0.05 (89).

244

245   To detect selective sweeps, we computed the cross-population extended haplotype homozygosity (XP-

246   EHH, (86) using the R package *rehh* (90). First, we phased the vcf files containing only the variant sites in

247   50-Kb windows using Shapeit v2.r904 (91). The XP-EHH is based on the comparison of haplotype lengths

248   between populations and has most detection power when the selected haplotype is near fixation in one

249   population and still polymorphic in the other. The genomic regions showing a –log10(p-value) ≥ 3 were

250   considered to be under selection. Then, we looked for overlapping regions between the F_{ST} and the XP-

251   EHH outliers. We generated Manhattan plots for all the statistics using the R package *qqman* (92) in R v.

252   3.6 (93).

253

254   ***Detecting putative chromosomal inversions***

255   In order to detect potential chromosomal inversions, we examined how patterns of population structure

256   varied along the genome using the R package *lostruct* (94). SNP data for each species including only

257   variant sites was converted to BCF format using BCFTOOLS version 1.9 (75). We implemented the script

258   provided by Huang et al., (95)dividing the genome into 1,000-SNP non-overlapping windows and

259   applying a principal components analysis (PCA) to each window. Euclidian distances between the two

260   first principal components (PCs) between windows were calculated and mapped using multidimensional

261   scaling (MDS) into a 40-dimensional space in order to see the similarity of the relatedness patterns

262   between windows. To identify genomic regions with extreme MDS values, windows with absolute values

263   greater than 4 SD over the mean across all windows were selected for each MDS coordinate. We

264   performed 1,000 permutations of windows over chromosomes to test if outlier regions were randomly

265   distributed across chromosomes. The putative inversion coordinates were the start position of the first

266   outlier window and the end position of the last outlier window. The script included additional analyses

267   to check if the MDS outliers were detecting inversions or instead other processes such as linked

268   selection. First, a PCA was performed using the SNPs from each putative inversion with *SNPRelate* (96).

269   Inversions in the PCA would split the samples into three different groups (i.e., the two orientations and

270   the heterozygotes in an intermediate cluster). The R function *kmeans* with the Hartigan & Wong (97)

271   method was used to identify the composition of groups of genotypes by performing clustering on the

272   first PC, setting the initial cluster centers as the maximum, minimum and middle of the PC score range.

273   Then, another test was performed averaging the individual heterozygosity per group detected by the k-

274   means clustering. Inversions would show a pattern of higher heterozygosity of the central group relative

275   to the other two groups. Finally, only MDS outlier regions that clustered into three groups in the PCA

276   and showed higher heterozygosity in the middle group were considered as putative inversions.

277

278   ***Candidate genes and GO-term enrichment analysis***

279   We extracted the candidate genes of the genomic regions detected to be under selection by both

280   methods separately (F_{ST} and XP-EHH outliers) using bedtools intersect and the annotation of their

281   respective reference genomes. We checked their functions in *genecards* (98). We obtained the GO

282   terms using the zebra finch dataset in *biomaRt* in R. We then performed a Gene ontology (GO)

283   enrichment analysis for each set of outliers in the category "biological function" using the *TopGO* R

284   package (99). To estimate the statistical significance, we used the Fisher exact test implementing the

285   *weight01* method. As recommended by the *TopGO* authors, we did not implement corrections for

286   multiple testing and presented raw p-values for the top-10 GO terms related to biological processes.

287

288   **Results**

289   ***Morphological differences***

290   The morphological analysis revealed marked differences in most traits between insular and continental

291   populations for all species. The small species (common chaffinch, junco and house finch), shared a

292   pattern of significantly larger values for most traits in the insular populations compared to mainland,

293   except for the junco wing length, which was longer in the continent (Table S3). In the larger sized red-

294   billed chough, we detected the opposite pattern, with significantly smaller values for most

295   morphological traits in the insular populations, except for bill width, which was smaller in the continent

296   (Table S3). The PC1 for all species showed significant differences among insular and mainland

297   populations, explaining over 39% of the variance in all cases (Fig. 2).

298

299   ***Whole-genome resequencing***

300   The total number of sites obtained in the variant calling was close to the length of the reference

301   genomes. The number of variant sites (40-50 million) was similar for all species except for the red-billed

302   chough, which was lower (~13 million), and the same pattern was maintained after filtering (Table S4).

303   The lower number of variants of the red-billed chough is consistent with its recent divergence, although

304   the house finch shows a high level of polymorphism, comparable to the other two species that diverged

305   a longer time ago.

306   ***Inference of demographic history***

307   PSMC-based demographic inference revealed a consistent pattern for the four species, showing stable

308   or growing effective population sizes for mainland populations and a sharp reduction in effective

309   population size in insular populations following colonization. The island-mainland divergence time

310   estimates obtained from the PSMC analysis are around 900,000 years for the common chaffinch,

311   100,000 years for the house finch, 400,000 years for the dark-eye junco, and 30,000 years for the red-

312   billed chough (Fig. 3, S2). The continental population of the red-billed chough showed the smallest

313   effective population size, and the smallest difference between the continental and insular populations

314   among the study species.

315

316   ***Inferring parallel evolution from genome-wide scans***

317   Genome-wide scans of genetic differentiation showed high heterogeneity across the four target species.

318   The F_{ST} genomic landscapes varied strongly among species (Fig. 4-7). Mean F_{ST} was higher in the common

319   chaffinch, followed by the dark-eyed junco, as expected for relatively longer island-mainland divergence

320   times. The red-billed chough showed a slightly higher mean F_{ST} than the house finch (Table 1). The red-

321   billed chough's genetic diversity was one order of magnitude lower than the rest, both for insular and

322   mainland populations. The insular common chaffinch population showed the second lowest genetic

323   diversity while the continental population showed the highest diversity value (Table 1). All species

324   showed consistently higher gene content and recombination rates at microchromosomes, and in

325   general, recombination rates were higher at chromosome extremes (Fig. 4-7).

326

327   The red-billed chough genomic landscape shows high levels of relative differentiation across the whole

328   genome with few outlier regions. Mean genetic diversity in both populations is one order of magnitude

329   lower than in the other three species (Table 1), showing very low values across the entire genome

330   except in the microchromosomes, where genetic diversity and divergence show higher values at regions

331   of high gene content. However, the XP-EHH analysis revealed evidence of selective sweeps, showing a

332   few clear peaks along the genome that coincide with drops in Tajima's D (Fig.4).

333

334   The common chaffinch genome landscape is characterized by several F_{ST} peaks that coincide with valleys

335   in d_{xy} and π, and peaks in Tajima's D mainly in the continent (i.e., peaks in chromosomes 1,1A, 2, 3, 4,

336   4A, 6, Fig. 5). This pattern is consistent with the model of recurrent selection, which states that selection

337   in the ancestor previous to the mainland-island split, generates a pattern of low d_{xy} and subsequent

338   selection after divergence reduces genetic diversity, generating F_{ST} peaks. XP-EHH detected selective

339   sweeps mostly concentrated in the microchromosomes and the Z chromosome; few of them coincided

340   with F_{ST} peaks.

341

342   The dark-eyed junco genomic landscape is highly differentiated across the entire genome, and there are

343   few outlier genomic regions, which often coincide with chromosomal extremes (Fig. 6). The XP-EHH

344   scans did not detect significant selective sweeps across the genome, with only three small regions

345   detected.

346

347   The house finch genomic landscape is characterized by a large, highly differentiated region in the middle

348   of chromosome 3, representing 47 million base pairs, suggesting a large chromosomal inversion. It

349   coincides with high values of Tajima's D in the continental population and a region of low

350   recombination, while d_{xy} and π show regular values (Fig. 7). At the end of the same chromosome and at

351   the beginning of chromosome 4, there are two F_{ST} peaks that coincide with a valley in d_{xy} and π, and a

352   peak in Tajima's D. This pattern is consistent with the recurrent selection model. The

353   microchromosomes show high relative differentiation along with high recombination rates and enriched

354   gene content. The XP-EHH scan showed a relatively flat landscape with no evidence for significant

355   selective sweeps.

356

Detecting putative chromosomal inversions

After combining all possible evidence, the analysis to detect inversions revealed that the red-billed chough genome has no putative inversions. The dark-eyed junco genome showed two possible inverted regions in chromosomes 6 and 7 (Table S5, Fig. S3A) but neither of them coincided with an F_{ST} outlier region. The common chaffinch genome showed two possible inversions in chromosomes 2 and 4, and both coincided with F_{ST} outlier regions (Table S5, Fig. S3B). The house finch genome revealed five putative inversions, a large one in chromosome 3, one in chromosome 1A, and three in chromosome 1. (Table S5, Fig. S3C). Only the large inversion in chromosome 3 coincides with an F_{ST} outlier region (Fig. 7).

Detection of candidate genes and GO-term enrichment analysis

Sharing of candidate genes among species was limited. There were only two genes putatively under selection that were shared between two species: the *morc2* gene was shared between the house finch and the dark-eyed junco, and the *spef2* gene was shared between the dark-eyed junco and the common chaffinch. The *morc2* gene is associated with Marie-Tooth Disease, Axonal, Type 2z (CMT2Z) and Developmental Delay, Impaired Growth, Dysmorphic Facies, and Axonal Neuropathy (DIGFAN) diseases in humans. CMT2Z is characterized by distal lower limb muscle weakness and sensory impairment (100) and DIFGAN by impaired motor and intellectual development, poor overall growth, usually short body height and microcephaly and subtly dysmorphic facial features in humans (101,102). The *spef2* gene is involved in sperm development and also plays a role in osteoblast differentiation, being required for normal bone growth (102).

In the red-billed chaough, the F_{ST} outliers mapped to 19 genes and the XP-EHH outliers detected selective sweeps in 14 genes, without overlap between the two methods. Due to the high relative differentiation across the genome and the absence of clear F_{ST} peaks, the clear selective sweeps along the genome could be a better approach to detect candidates for the red-billed chough. However, most of the genes among the 14 outlier genes found within sweeps have unknown functions, and only five genes have known functions and associated GO terms. From the 20,580 available genes from the *Corvus moneduloides* genome, only 8,632 from the gene universe (including the five significant genes) could be used for the analysis. Among the top-10 GO terms for the XP-EHH outliers we found several related to

386   chromatin cohesion (i.e., regulation of cohesion loading and negative regulation of sister chromatid

387   cohesion) (Table S6).

388

389   In the common chaffinch, the genomic scan detected 85 genes in the F_{ST} outlier regions, and the XP-EHH

390   revealed 1,724 outliers that mapped to 21 genes, 3 of which were shared with the F_{ST} candidates. Among

391   the 16,563 genes available in the gene universe, the GO term analysis detected 9,065 feasible genes,

392   including 48 out of the 85 significant genes detected as F_{ST} outliers. Among the top-10 GO terms we

393   found several involved in transcription regulation such as "transcription-dependent tethering of RNA

394   polymerase II gene DNA at nuclear periphery" and "histone H3-K4 acetylation", and others affecting

395   translation like "lysyl-tRNA aminoacylation" (Table S7). There were also two terms related to cell

396   adhesion "regulation of protein localization to cell-cell adherens junction" and "regulation of focal

397   adhesion assembly", as well as two terms associated with the organization of cellular components

398   including: "positive regulation of endosome organization" and "lysosome localization".

399

400   In the dark-eyed junco, the F_{ST} genome scan detected relatively few peaks distributed across the genome

401   that mapped to 24 genes, and three regions were detected as sweeps by the XP-EHH scan but did not

402   contain known genes. Among the 24 genes, only 16 had GO terms associated with them. The GO

403   enrichment analysis performed with a gene universe of 17,038 genes found 9,220 feasible genes

404   including 15 potential candidate genes. The top-10 GO terms revealed three terms related to the

405   centrosome, including "negative regulation of protein localization to centrosome", "protein localization

406   to pericentriolar material" and "positive regulation of mitotic centrosome separation" (Table S8).

407

408   Finally, in the house finch, the F_{ST} genome scan detected 111 genes putatively under selection, while the

409   XP-EHH scan detected no significant outliers. From the genes identified under selection, 20 were

410   clustered in the middle region of chromosome 3, and two were at the end of the same chromosome.

411   The remaining genes were mainly clustered within microchromosomes. From the 16,563 available genes

412   in the gene universe, 9,065 including 83 significant genes could be used in the GO enrichment analysis.

413   Within the top-10 significant GO terms (Table S9) we find "growth plate cartilage chondrocyte

414   morphogenesis" which is involved in skeletal development and morphogenesis. Also involved in

415   morphogenesis we found the term "zonula adherens maintenance" which is related to cell-cell

416   adhesion. We also find several terms associated with transcription, including "negative regulation of

417 telomerase RNA reverse transcriptase activity", "glutaminyl-tRNA aminoacylation" and two histone

418 acetylations (H2-K14 and H3-K23).

419

420 **Discussion**

421 Our comparative analysis of mainland and insular populations of four passerine species yielded shared

422 patterns of phenotypic divergence and demographic history, in contrast to species-specific patterns of

423 related genome-wide variation. Relative to the mainland, all insular populations showed changes in

424 body size, and suffered reductions in effective population size and genetic diversity, patterns that are

425 consistent with previous findings (13,48,103). Island colonizations are usually initiated by a small group

426 of individuals, and the resulting genetic drift, combined with the small size of the island's geographic

427 area, leads to a small effective population size and low genetic diversity (48,104). Among the four

428 species, the red-billed chough showed the smallest effective population size in both insular and

429 mainland populations, which corresponds to the lowest levels of genetic diversity. In the mainland, this

430 species has shown marked levels of genetic structure in the absence of geographic barriers, suggesting

431 that social barriers due to complex behavioral interactions may constrain gene flow and thus the

432 effective size of local populations (105); the insular population is unlikely to be an exception (60).

433

434 Using PC1 and mean differences in tarsus length, as proxies for structural body size in birds (106–109),

435 we found that the three smaller passerines increased in size and the larger species suffered a size

436 reduction upon island colonization. This is consistent with the island rule, which posits that small birds

437 evolve towards a larger size and large birds towards a smaller size upon island colonization (12,13).

438 However, the difference in the house finch tarsus length among insular and mainland populations was

439 not significant probably due to the small sample size. Regarding beak size, we find that insular

440 individuals from the small sized and short-billed species show longer bills than their mainland

441 counterparts whereas the insular population of the long-billed chough species shows a reduction in bill

442 length. All the species show also differences in at least other bill dimension; however, the red billed

443 chough is the only one in which the change is in the opposite direction, showing shorter but wider bills

444 on the island. The beak is both a feeding and thermoregulatory structure with great evolutionary

445 potential that allows birds to quickly adapt to new environmental conditions (110) and therefore plays a

446 fundamental role in avian fitness (111–116).

447

448   A major question in evolutionary biology is whether shared phenotypic traits are the result of

449   evolutionary convergence, and the degree to which traits under similar selective pressures share a

450   common genetic basis (117,118). Finding shared patterns of genomic variation and common regions of

451   divergence at the intra- or inter-specific levels has been of major interest to understand the mechanisms

452   underlying local adaptation (43,49,50). These shared divergent regions across taxa are particularly

453   interesting when differentiation evolved independently in unrelated lineages (53). A striking result of

454   our comparative analysis of island-mainland populations in four passerine species is the lack of

455   parallelism in their respective genomic landscapes. We found highly differentiated genomic regions in all

456   four species that were often associated with reduced genetic diversity, suggesting the role of selection

457   in island-mainland differentiation. Yet the lack of congruence in the location of these regions along the

458   genome indicates that the four species adapted to insular environments in different ways, through

459   genetic changes at different loci. Moreover, patterns of recombination rate in these regions suggest that

460   the genomic mechanisms generating these patterns, which include selective sweeps caused by

461   directional selection, chromosomal inversions, and historical factors like recurrent selection, differ in

462   each of the four species.

463

464   According to our demographic analysis, the divergence between red-billed choughs on La Palma and the

465   Iberian Peninsula took place around 30,000 years ago, considering a generation time of two years. A

466   previous study (60) estimated the divergence event in a similar time range, within the last 10,000 years

467   using mitochondrial data and around 30,000 years using iMA2, however they used a generation time of

468   6 years based on mainland data. If we apply that value, the divergence time estimate changes to around

469   110,000 years. The red-billed chough also shows the smallest effective population size lowest genetic

470   diversity. This reduced genetic diversity also results in an inflation of the relative divergence (29,119),

471   causing a high baseline to detect outliers while the absolute divergence remains low. The recent

472   divergence of the red-billed chough is apparent due to the low divergence along the genome with a

473   mean d_{xy} value of $8.2 \cdot 10^{-4}$. The regions of higher divergence and genetic diversity are located in the

474   microchromosomes, which have relatively higher recombination rates and higher gene content (120).

475   However, the scan for selective sweeps, which is more efficient in detecting recent divergence, revealed

476   clear peaks along the genome. The red-billed chough is the species showing the strongest selective

477   sweeps, which is also consistent with the low genetic diversity of the species due to genomic hitchhiking

478   of the sites flanking selected loci (121). Among the top ten GO terms of the genes within the selective

479   sweeps there were several related with chromatin cohesion. Specifically, the WAPL gene negatively

480 regulates the association of cohesin with chromatin, having an opposing function to the NIPBL gene.

481 Mutations in the NIPBL gene cause Cornelia de Lange syndrome (CdLS), therefore, mutations in WAPL

482 gene could generate similar developmental deficits to CdLS (122). CdLS can affect most organ systems,

483 but typical characters include craniofacial structures, upper extremities, eyes and the gastrointestinal

484 system (123,124). The actual role of WAPL has not been properly tested, but it has been associated with

485 Warsaw Breakage Syndrome (WABS) (125), which is a cohesinopathy that causes growth retardation,

486 severe microcephaly, sensorineural hearing loss, cochlear anomalies, intellectual disability and abnormal

487 skin pigmentation (125,126).

488

489 The common chaffinch of La Palma was found to have diverged from its mainland relatives around 0.8-

490 0.9 my ago, which is in agreement with previous reconstructions of the species evolutionary history (61).

491 A study of the entire common chaffinch radiation across the Atlantic archipelagos revealed that it first

492 colonized Azores, then Madeira and finally the Canary Islands (61). This sequential colonization of

493 isolated archipelagos has left a genomic signature of recurrent selection along the genome, leading to

494 regions with low absolute divergence due to selection in the ancestor, that were subsequently selected

495 in the daughter populations, reducing genetic diversity and generating F_{ST} peaks (45). This recurrent-

496 selection model fits well with the known colonization history, as the first selective episode probably

497 occurred upon colonization of the Azores, and then at every subsequent colonization step between

498 islands, where successive selective events at the same genomic regions likely led to a loss of genetic

499 diversity. Among the genes associated with outlier loci there were several involved in metabolism (i.e.,

500 *fabp2*, *kars1*, *lipa*, *nfrkb*, *pdha1*), five involved in pigmentation and six related to singing. Among the

501 genes related to pigmentation, there were several related to avian plumage coloration, *ap3b1* (127),

502 *hps6* (128) and *ric1* (129), one was related to sexual dichromatism in birds (130), and the *atrn* gene was

503 related to melanin production and has also been associated with coat coloration in macaques (131).

504 Regarding the genes related to song, we detected, *chrm2* and *chrm5*, which have shown differential

505 expression associated with song learning and production in zebra finch (132), the mrps27 (133) and

506 *upf3b* (134), which are involved in the song control system in the zebra finch, the *paip1* gene, which has

507 been associated with song learning (135), and the *ube2d3* gene, which was related to musical abilities

508 using a convergent evidence method including data from humans, songbirds and other animals (136).

509 Interestingly, within the top-ten significant GO terms we detected "positive regulation of endosome

510 organization" and endosomes play an important role in neural development (137). We also find the

511 term "regulation of focal adhesion assembly" and it has been shown that cell adhesion plays an

512 important role in tissue morphogenesis (138).

513

514 In the dark-eyed junco, the demographic inference revealed that the insular population on Guadalupe

515 diverged around 400,000 years ago, which is similar to previous estimates (59). The differentiated

516 regions were mainly distributed at the ends of chromosomes, coinciding with telocentric centromeres,

517 as previously found in Swainson's thrushes (139). Consistent with this pattern, among the top-ten GO

518 terms we identified several that were related to the centrosomes, increasingly recognized as signaling

519 machines capable of regulating many cellular functions (140).

520

521 In the house finch, the genomic landscape showed signatures of different processes. Despite the recent

522 divergence time between mainland and Guadalupe Island populations, estimated at about 100,000

523 years before present, we did no detect signatures of significant selective sweeps. The large region

524 showing high differentiation and very low recombination in chromosome 3 likely represents a major

525 chromosomal inversion. Genomic islands of differentiation could be generated by chromosomal

526 rearrangements that cluster highly differentiated loci together due to genomic hitchhiking (95,141).

527 However, that could represent either a group of adaptive alleles or several neutral loci linked to a focal

528 selected allele (141). Several studies have found regions highly diverged within chromosomal inversions

529 (95,142–144). In this case, 20 genes putatively under selection were found within the inversion. Two of

530 those genes (*fam162b* and *fig4*) are related to facial morphology and related disorders. Little is known

531 about the function of the *fam162b* gene, but it is expressed in mouse facial prominences (145), and *fig4*

532 is associated with the Yunis-Varon syndrome, characterized by skeletal defects including cleidocranial

533 dysplasia, digital anomalies and neurological impairment (146,147). Another interesting candidate is the

534 *lyd* gene, which is also found within an inversion in chromosome 2 in the white-throated sparrow

535 (*Zonotrichia albicollis*) and has shown differences in expression between two morphs that differed in

536 territorial aggression including song (147). Within that inversion, they found mainly genes related to

537 behavior and plumage color. Some genes within the inversion in the house finch are related to mental

538 retardation in humans including FMN2 (148,149), or to behavior in mice, like *pnisr* (150,151).

539 Interestingly, within the house finch inversion we also found the gene *gtf3c6*, which was found to be a

540 candidate involved in sexual selection in a comparison of 11 bird genomes (151). Within the top-ten

541 significant GO terms, we found "growth plate cartilage chondrocyte morphogenesis", which is involved

542 in skeletal development and morphogenesis and regulated by multiple signaling pathways including,

543   among others, the bone morphogenetic proteins (Bmp; (152), fibroblast growth factors (FGFs; (153) and

544   Wingless/int.1 molecules (Wnt; (154). Among these pathways, the Bmp and Wnt signaling pathways are

545   known to be involved in facial development in different organisms including beak morphology in birds

546   (155,156). We also found the term "zonula adherens maintenance" and it has been shown that the

547   adherens junctions are also involved in tissue morphogenesis (138).

548

549   Here we studied four cases of island-mainland divergence in passerine species that have colonized

550   oceanic islands and share phenotypic modifications likely caused by similar selective pressures, and

551   asked whether the underlying genetic mechanisms were also shared. Our general result in this respect is

552   that the regions of the genome showing evidence of divergence under directional selection are lineage

553   specific, suggesting that the genetic basis of phenotypic divergence is different in each case, so that

554   evidence for convergence at the genomic level appears to be lacking (49). Even if the same regions had

555   been detected as putatively under selection or with shared genomic features involved in genomic

556   differentiation, such as the stable recombination landscape in avian lineages (56), it would be difficult to

557   determine whether that pattern is generated by directional selection or by background and linked

558   selection. Despite examples showing that few loci of large effect can drive adaptive divergence in

559   complex traits, such as the bill (e.g., (157), selection is likely to act on many loci of small effect due to the

560   polygenic nature of most adaptive traits (158,159). Consequently, convergent phenotypes could in fact

561   be due to divergent genotypes. Several examples to date show that phenotypic change in a given trait

562   can be driven by different sets of genes, such as mouth morphology in cichlid fishes (160), or color

563   pattern in mice (161,162) and flies (163). Even though the outlier genes differ among species, there

564   could be common significant GO terms because different genes share functions and pathways.

565   Interestingly, between the common chaffinch and the house finch we found several similar GO terms

566   related to tRNA aminoacylation, histone acetylations and cell adherens junctions. Remarkably, we found

567   that in all four species, GO terms are mostly related to gene regulation, for instance by modifying

568   histones or altering chromatin binding and chromosome condensation, which are essential for

569   differentiation and development. Recently, Monroe et al. (164)reported that mutations occur less often

570   in functional regions of the genome, and that epigenomic and physical chromosomal features account

571   for the position of the mutations. In our case, most of the terms related to outlier loci are involved in

572   epigenetic modifications, suggesting that changes in gene regulation, instead of specific core genes, may

573   be the main drivers of divergence. Currently, several models are being developed to understand the role

574   of gene regulation in the evolution of complex traits (27,165), implying that regulatory regions are

575 disproportionately targeted by polygenic selection, highlighting the key role of gene regulatory networks

576 in evolution (166).

577

Declarations

Consent for publication

Not Applicable

Ethics approval and consent to participate

Project compliant with CSIC animal welfare regulations and approved by CSIC's Ethics Committee (Ref. 1415/2023). Field sampling was carried out in compliance with ethical and research guidelines under permits A/EST-004/2020 and A/EST-003/2021 from the Cabildo de La Palma, Canarian Regional Government.

Availability of data and materials

Resequencing raw data is deposited at NCBI under the SRA data projects PRJNA661201 (for common chaffinch mainland population) with accession numbers SAMN16094451-SAMN16094459 and PRJNA1077913 with accession numbers SAMN39984864- SAMN39984947, for the common chaffinch insular population and both populations from the rest of the species, see Table S1 for details) and the datasets, are deposited in Figshare (https://doi.org/10.6084/m9.figshare.21590673).

Competing interests

No competing interests

Authors' contributions

MR carried out the molecular lab work, carried out the data curation and analysis, participated in the design of the study, collected field data and drafted the manuscript; JM collected field data and critically

602 revised the manuscript; GB conceived and designed the study, collected field data and critically revised

603 the manuscript; BM conceived and designed the study, collected field data and critically revised the

604 manuscript. All authors gave final approval for publication and agree to be held accountable for the

605 work performed therein.

606 **Acknowledgements**

608

609 **References**

610

611 1. Schluter D. The ecology of adaptive radiation. OUP Oxford; 2000.
612 2. Grant PR. Reconstructing the evolution of birds on islands: 100 years of research. Oikos.
613   2001;92(3):385–403.
614 3. Price T. Speciation in birds. Roberts and Company. greenwood Village, CO; 2008.
615 4. Warren BH, Simberloff D, Ricklefs RE, Aguilée R, Condamine FL, Gravel D, et al. Islands as model
616   systems in ecology and evolution: prospects fifty years after MacArthur-Wilson. Ecol Lett.
617   2015;18(2):200–17.
618 5. Gillespie RG, Bennett GM, De Meester L, Feder JL, Fleischer RC, Harmon LJ, et al. Comparing
619   adaptive radiations across space, time, and taxa. Journal of Heredity. 2020;111(1):1–20.
620 6. Grant PR, Grant BR. Adaptive radiation of Darwin's finches: Recent data help explain how this
621   famous group of Galapagos birds evolved, although gaps in our understanding remain. Am Sci.
622   2002;90(2):130–9.
623 7. Losos JB, Ricklefs RE. Adaptation and diversification on islands. Nature. 2009;457(7231):830–6.
624 8. Brown RM, Siler CD, Oliveros CH, Esselstyn JA, Diesmos AC, Hosner PA, et al. Evolutionary
625   processes of diversification in a model island archipelago. Annu Rev Ecol Evol Syst. 2013;44:411–
626   35.
627 9. Woolfit M, Bromham L. Population size and molecular evolution on islands. Proceedings of the
628   Royal Society B: Biological Sciences. 2005;272(1578):2277–82.
629 10. Whittaker RJ, Fernández-Palacios JM, Matthews TJ, Borregaard MK, Triantis KA. Island
630   biogeography: taking the long view of nature's laboratories. Science (1979).
631   2017;357(6354):eaam8326.
632 11. Foster JB. Evolution of mammals on islands. Nature. 1964;202(4929):234–5.
633 12. Clegg SM, Owens PF. The 'island rule'in birds: medium body size and its ecological explanation.
634   Proc R Soc Lond B Biol Sci. 2002;269(1498):1359–65.
635 13. Benítez-López A, Santini L, Gallego-Zamorano J, Milá B, Walkden P, Huijbregts MAJ, et al. The
636   island rule explains consistent patterns of body size evolution in terrestrial vertebrates. Nat Ecol
637   Evol. 2021;5(6):768–86.
638 14. Sackton TB, Clark N. Convergent evolution in the genomics era: new insights and directions. Vol.
639   374, Philosophical Transactions of the Royal Society B. The Royal Society; 2019. p. 20190102.
640 15. Clegg S. Evolutionary changes following island colonization in birds. The theory of island
641   biogeography revisited. 2010;293–325.

642 16. Rosenblum EB, Parent CE, Brandt EE. The molecular basis of phenotypic convergence. Annu Rev
643   Ecol Evol Syst. 2014;45:203–26.
644 17. Blondel J. Evolution and ecology of birds on islands: trends and prospects. Vie et Milieu/Life &
645   Environment. 2000;205–20.
646 18. Sayol F, Downing PA, Iwaniuk AN, Maspons J, Sol D. Predictable evolution towards larger brains in
647   birds colonizing oceanic islands. Nat Commun. 2018;9(1):2820.
648 19. Lapiedra O, Sayol F, Garcia-Porta J, Sol D. Niche shifts after island colonization spurred adaptive
649   diversification and speciation in a cosmopolitan bird clade. Proceedings of the Royal Society B.
650   2021;288(1958):20211022.
651 20. Glor RE, Gifford ME, Larson A, Losos JB, Schettino LR, Lara ARC, et al. Partial island submergence
652   and speciation in an adaptive radiation: a multilocus analysis of the Cuban green anoles. Proc R
653   Soc Lond B Biol Sci. 2004;271(1554):2257–65.
654 21. Campana MG, Corvelo A, Shelton J, Callicrate TE, Bunting KL, Riley-Gillis B, et al. Adaptive
655   radiation genomics of two ecologically divergent Hawai 'ian honeycreepers: the 'akiapōlā 'au and
656   the Hawai 'i 'amakihi. Journal of Heredity. 2020;111(1):21–32.
657 22. Blanco G, Laiolo P, Fargallo JA. Linking environmental stress, feeding-shifts and the 'island
658   syndrome': a nutritional challenge hypothesis. Popul Ecol. 2014;56:203–16.
659 23. Tattersall GJ, Chaves JA, Danner RM. Thermoregulatory windows in Darwin's finches. Funct Ecol.
660   2018;32(2):358–68.
661 24. Manceau M, Domingues VS, Linnen CR, Rosenblum EB, Hoekstra HE. Convergence in
662   pigmentation at multiple levels: mutations, genes and function. Philosophical Transactions of the
663   Royal Society B: Biological Sciences. 2010;365(1552):2439–50.
664 25. Reed RD, Papa R, Martin A, Hines HM, Counterman BA, Pardo-Diaz C, et al. Optix drives the
665   repeated convergent evolution of butterfly wing pattern mimicry. Science (1979).
666   2011;333(6046):1137–41.
667 26. Colosimo PF, Hosemann KE, Balabhadra S, Villarreal Jr G, Dickson M, Grimwood J, et al.
668   Widespread parallel evolution in sticklebacks by repeated fixation of ectodysplasin alleles.
669   Science (1979). 2005;307(5717):1928–33.
670 27. Boyle EA, Li YI, Pritchard JK. An expanded view of complex traits: from polygenic to omnigenic.
671   Cell. 2017;169(7):1177–86.
672 28. Sendell-Price AT, Ruegg KC, Robertson BC, Clegg SM. An island-hopping bird reveals how founder
673   events shape genome-wide divergence. Mol Ecol. 2021;30(11):2495–510.
674 29. Cruickshank TE, Hahn MW. Reanalysis suggests that genomic islands of speciation are due to
675   reduced diversity, not reduced gene flow. Mol Ecol. 2014;23(13):3133–57.
676 30. Burri R. Interpreting differentiation landscapes in the light of long-term linked selection. Evol
677   Lett. 2017;1(3):118–31.
678 31. Ravinet M, Faria R, Butlin RK, Galindo J, Bierne N, Rafajlović M, et al. Interpreting the genomic
679   landscape of speciation: a road map for finding barriers to gene flow. J Evol Biol.
680   2017;30(8):1450–77.
681 32. Feng S, Stiller J, Deng Y, Armstrong J, Fang QI, Reeve AH, et al. Dense sampling of bird diversity
682   increases power of comparative genomics. Nature. 2020;587(7833):252–7.
683 33. Chase MA, Ellegren H, Mugal CF. Positive selection plays a major role in shaping signatures of
684   differentiation across the genomic landscape of two independent Ficedula flycatcher species
685   pairs. Evolution (N Y). 2021;75(9):2179–96.
686 34. Ellegren H, Smeds L, Burri R, Olason PI, Backström N, Kawakami T, et al. The genomic landscape
687   of species divergence in Ficedula flycatchers. Nature. 2012;491(7426):756–60.

688   35.   Nadeau NJ, Whibley A, Jones RT, Davey JW, Dasmahapatra KK, Baxter SW, et al. Genomic islands
689   of divergence in hybridizing Heliconius butterflies identified by large-scale targeted sequencing.
690   Philosophical Transactions of the Royal Society B: Biological Sciences. 2012;367(1587):343–53.

691   36.   Poelstra JW, Vijay N, Bossu CM, Lantz H, Ryll B, Müller I, et al. The genomic landscape underlying
692   phenotypic integrity in the face of gene flow in crows. Science (1979). 2014;344(6190):1410–4.

693   37.   Meier JI, Marques DA, Wagner CE, Excoffier L, Seehausen O. Genomics of parallel ecological
694   speciation in Lake Victoria cichlids. Mol Biol Evol. 2018;35(6):1489–506.

695   38.   Turner TL, Hahn MW, Nuzhdin S V. Genomic islands of speciation in Anopheles gambiae. PLoS
696   Biol. 2005;3(9):e285.

697   39.   Weir BS, Cockerham CC. Estimating F-statistics for the analysis of population structure. Evolution
698   (N Y). 1984;1358–70.

699   40.   Nosil P, Funk DJ, Ortiz-Barrientos D. Divergent selection and heterogeneous genomic divergence.
700   Mol Ecol. 2009;18(3):375–402.

701   41.   Zeng K, Corcoran P. The effects of background and interference selection on patterns of genetic
702   variation in subdivided populations. Genetics. 2015;201(4):1539–54.

703   42.   Feder JL, Nosil P. The efficacy of divergence hitchhiking in generating genomic islands during
704   ecological speciation. Evolution (N Y). 2010;64(6):1729–47.

705   43.   Burri R, Nater A, Kawakami T, Mugal CF, Olason PI, Smeds L, et al. Linked selection and
706   recombination rate variation drive the evolution of the genomic landscape of differentiation
707   across the speciation continuum of Ficedula flycatchers. Genome Res. 2015;25(11):1656–65.

708   44.   Irwin DE, Milá B, Toews DPL, Brelsford A, Kenyon HL, Porter AN, et al. A comparison of genomic
709   islands of differentiation across three young avian species pairs. Mol Ecol. 2018;27(23):4839–55.

710   45.   Irwin DE, Alcaide M, Delmore KE, Irwin JH, Owens GL. Recurrent selection explains parallel
711   evolution of genomic regions of high relative but low absolute differentiation in a ring species.
712   Mol Ecol. 2016;25(18):4488–507.

713   46.   Han F, Lamichhaney S, Grant BR, Grant PR, Andersson L, Webster MT. Gene flow, ancient
714   polymorphism, and ecological adaptation shape the genomic landscape of divergence among
715   Darwin's finches. Genome Res. 2017;27(6):1004–15.

716   47.   Ferchaud A, Hansen MM. The impact of selection, gene flow and demographic history on
717   heterogeneous genomic divergence: Three-spine sticklebacks in divergent environments. Mol
718   Ecol. 2016;25(1):238–59.

719   48.   Leroy T, Rousselle M, Tilak MK, Caizergues AE, Scornavacca C, Recuerda M, et al. Island songbirds
720   as windows into evolution in small populations. Current Biology. 2021;31(6):1303–10.

721   49.   Van Doren BM, Campagna L, Helm B, Illera JC, Lovette IJ, Liedvogel M. Correlated patterns of
722   genetic diversity and differentiation across an avian family. Mol Ecol. 2017;26(15):3982–97.

723   50.   Delmore KE, Lugo Ramos JS, Van Doren BM, Lundberg M, Bensch S, Irwin DE, et al. Comparative
724   analysis examining patterns of genomic differentiation across multiple episodes of population
725   divergence in birds. Evol Lett. 2018;2(2):76–87.

726   51.   Vijay N, Weissensteiner M, Burri R, Kawakami T, Ellegren H, Wolf JBW. Genomewide patterns of
727   variation in genetic diversity are shared among populations, species and higher-order taxa. Mol
728   Ecol. 2017;26(16):4284–95.

729   52.   Carbeck K, Arcese P, Lovette I, Pruett C, Winker K, Walsh J. Candidate genes under selection in
730   song sparrows co-vary with climate and body mass in support of Bergmann's Rule. Nat Commun.
731   2023;14(1):6974.

732   53.   Seehausen O, Butlin RK, Keller I, Wagner CE, Boughman JW, Hohenlohe PA, et al. Genomics and
733   the origin of species. Nat Rev Genet. 2014;15(3):176–92.

734   54.   Zhang G, Li C, Li Q, Li B, Larkin DM, Lee C, et al. Comparative genomics reveals insights into avian
735   genome evolution and adaptation. Science (1979). 2014;346(6215):1311–20.

736 55. Ellegren H. Evolutionary stasis: the stable chromosomes of birds. Trends Ecol Evol.
737   2010;25(5):283–91.
738 56. Singhal S, Leffler EM, Sannareddy K, Turner I, Venn O, Hooper DM, et al. Stable recombination
739   hotspots in birds. Science (1979). 2015;350(6263):928–32.
740 57. Kawakami T, Mugal CF, Suh A, Nater A, Burri R, Smeds L, et al. Whole-genome patterns of linkage
741   disequilibrium across flycatcher populations clarify the causes and consequences of fine-scale
742   recombination rate variation in birds. Mol Ecol. 2017;26(16):4158–72.
743 58. Dutoit L, Burri R, Nater A, Mugal CF, Ellegren H. Genomic distribution and estimation of
744   nucleotide diversity in natural populations: perspectives from the collared flycatcher (Ficedula
745   albicollis) genome. Mol Ecol Resour. 2017;17(4):586–97.
746 59. Aleixandre P, Hernández Montoya J, Mila B. Speciation on oceanic islands: Rapid adaptive
747   divergence vs. cryptic speciation in a Guadalupe Island songbird (Aves: Junco). PLoS One.
748   2013;8(5):e63242.
749 60. Morinha F, Milá B, Dávila JA, Fargallo JA, Potti J, Blanco G. The ghost of connections past: A role
750   for mainland vicariance in the isolation of an insular population of the red-billed chough (Aves:
751   Corvidae). J Biogeogr. 2020;47(12):2567–83.
752 61. Recuerda M, Illera JC, Blanco G, Zardoya R, Milá B. Sequential colonization of oceanic
753   archipelagos led to a species-level radiation in the common chaffinch complex (Aves: Fringilla
754   coelebs). Mol Phylogenet Evol. 2021;164:107291.
755 62. Tuttle EM, Bergland AO, Korody ML, Brewer MS, Newhouse DJ, Minx P, et al. Divergence and
756   functional degradation of a sex chromosome-like supergene. Current Biology. 2016;26(3):344–
757   50.
758 63. Billerman M, Keeney BK, Rodewald PG, Schulenberg TS. Birds of the World. Cornell Lab of
759   Ornithology, Ithaca. 2022.
760 64. Griffiths R, Daan S, Dijkstra C. Sex identification in birds using two CHD genes. Proc R Soc Lond B
761   Biol Sci. 1996;263(1374):1251–6.
762 65. Milá B, Wayne RK, Smith TB. Ecomorphology of migratory and sedentary populations of the
763   yellow-rumped warbler (Dendroica coronata). Condor. 2008;110(2):335–44.
764 66. Blanco G, Tella JL, Torre I. Age and Sex Determination of Monomorphic Non-Breeding Choughs: A
765   Long-Term Study (Determinacion de la Edad y el Sexo en Chovas Piquirrojas Pyrrhocorax
766   pyrrhocorax no Reproductoras: un Estudio a Largo Plazo). J Field Ornithol. 1996;428–33.
767 67. Krueger F. TrimGalore: A wrapper tool around Cutadapt and FastQC to consistently apply quality
768   and adapter trimming to FastQ files. Babraham Bioinformatics. 2015.
769 68. Li H, Durbin R. Fast and accurate long-read alignment with Burrows–Wheeler transform.
770   Bioinformatics. 2010;26(5):589–95.
771 69. Recuerda M, Vizueta J, Cuevas-Caballé C, Blanco G, Rozas J, Milá B. Chromosome-level genome
772   assembly of the common chaffinch (Aves: Fringilla coelebs): a valuable resource for evolutionary
773   biology. Genome Biol Evol. 2021;13(4):evab034.
774 70. Friis G, Vizueta J, Ketterson ED, Milá B. A high-quality genome assembly and annotation of the
775   dark-eyed junco Junco hyemalis, a recently diversified songbird. G3. 2022;12(6):jkac083.
776 71. Danecek P, Bonfield JK, Liddle J, Marshall J, Ohan V, Pollard MO, et al. Twelve years of SAMtools
777   and BCFtools. Gigascience. 2021;10(2):giab008.
778 72. Danecek P, Auton A, Abecasis G, Albers CA, Banks E, DePristo MA, et al. The variant call format
779   and VCFtools. Bioinformatics. 2011;27(15):2156–8.
780 73. Marçais G, Delcher AL, Phillippy AM, Coston R, Salzberg SL, Zimin A. MUMmer4: A fast and
781   versatile genome alignment system. PLoS Comput Biol. 2018;14(1):e1005944.
782 74. Li H, Durbin R. Inference of human population history from individual whole-genome sequences.
783   Nature. 2011;475(7357):493–6.

784 75. Li H, Handsaker B, Wysoker A, Fennell T, Ruan J, Homer N, et al. The sequence alignment/map
785   format and SAMtools. bioinformatics. 2009;25(16):2078–9.
786 76. Wright AE, Mank JE. The scope and strength of sex-specific selection in genome evolution. J Evol
787   Biol. 2013;26(9):1841–53.
788 77. Nadachowska-Brzyska K, Burri R, Smeds L, Ellegren H. PSMC analysis of effective population sizes
789   in molecular ecology and its application to black-and-white Ficedula flycatchers. Mol Ecol.
790   2016;25(5):1058–72.
791 78. Smeds L, Qvarnström A, Ellegren H. Direct estimate of the rate of germline mutation in a bird.
792   Genome Res. 2016;26(9):1211–8.
793 79. Ericson PGP, Qu Y, Blom MPK, Johansson US, Irestedt M. A genomic perspective of the pink-
794   headed duck Rhodonessa caryophyllacea suggests a long history of low effective population size.
795   Sci Rep. 2017;7(1):16853.
796 80. Hanna ZR, Henderson JB, Wall JD, Emerling CA, Fuchs J, Runckel C, et al. Northern spotted owl
797   (Strix occidentalis caurina) genome: divergence with the barred owl (Strix varia) and
798   characterization of light-associated genes. Genome Biol Evol. 2017;9(10):2522–45.
799 81. Sato Y, Ogden R, Kishida T, Nakajima N, Maeda T, Inoue-Murayama M. Population history of the
800   golden eagle inferred from whole-genome sequencing of three of its subspecies. Biological
801   Journal of the Linnean Society. 2020;130(4):826–38.
802 82. Baker AJ, Marshall HD. Population divergence in Chaffinches Fringilla coelebs assessed with
803   control-region sequences. In: Proceedings XXII International Ornithological Congress (NJ Adams
804   and RH Slotow, Eds) BirdLife South Africa, Durban. 1999. p. 1899–913.
805 83. Reid JM, Bignal EM, Bignal S, McCracken DI, Monaghan P. Age-specific reproductive performance
806   in red-billed choughs Pyrrhocorax pyrrhocorax: patterns and processes in a natural population.
807   Journal of Animal Ecology. 2003;765–76.
808 84. Friis G, Aleixandre P, Rodríguez-Estrella R, Navarro-Sigüenza AG, Milá B. Rapid postglacial
809   diversification and long-term stasis within the songbird genus Junco: phylogeographic and
810   phylogenomic evidence. Mol Ecol. 2016;25(24):6175–95.
811 85. McVean G, Auton A. LDhat 2.1: a package for the population genetic analysis of recombination.
812   Department of Statistics, Oxford, OX1 3TG, UK. 2007;
813 86. Sabeti PC, Varilly P, Fry B, Lohmueller J, Hostetter E, Cotsapas C, et al. Genome-wide detection
814   and characterization of positive selection in human populations. Nature. 2007;449(7164):913–8.
815 87. Korunes KL, Samuk K. pixy: Unbiased estimation of nucleotide diversity and divergence in the
816   presence of missing data. Mol Ecol Resour. 2021;21(4):1359–68.
817 88. Tajima F. Statistical method for testing the neutral mutation hypothesis by DNA polymorphism.
818   Genetics. 1989;123(3):585–95.
819 89. Benjamini Y, Hochberg Y. Controlling the false discovery rate: a practical and powerful approach
820   to multiple testing. Journal of the Royal statistical society: series B (Methodological).
821   1995;57(1):289–300.
822 90. Gautier M, Klassmann A, Vitalis R. rehh 2.0: a reimplementation of the R package rehh to detect
823   positive selection from haplotype structure. Mol Ecol Resour. 2017;17(1):78–90.
824 91. Delaneau O, Zagury JF, Marchini J. Improved whole-chromosome phasing for disease and
825   population genetic studies. Nat Methods. 2013;10(1):5–6.
826 92. Turner SD. qqman: an R package for visualizing GWAS results using QQ and manhattan plots.
827   Biorxiv. 2014;005165.
828 93. Team RC, Team RC. R: a language and environment for statistical computing. R Found. Stat
829   Comput Vienna Austria. 2017;
830 94. Li H, Ralph P. Local PCA shows how the effect of population structure differs along the genome.
831   Genetics. 2019;211(1):289–304.

832 95. Huang K, Andrew RL, Owens GL, Ostevik KL, Rieseberg LH. Multiple chromosomal inversions
833   contribute to adaptive divergence of a dune sunflower ecotype. Mol Ecol. 2020;29(14):2535–49.
834 96. Zheng X, Levine D, Shen J, Gogarten SM, Laurie C, Weir BS. A high-performance computing
835   toolset for relatedness and principal component analysis of SNP data. Bioinformatics.
836   2012;28(24):3326–8.
837 97. Hartigan JA, Wong MA. Algorithm AS 136: A k-means clustering algorithm. J R Stat Soc Ser C Appl
838   Stat. 1979;28(1):100–8.
839 98. Rappaport N, Twik M, Plaschkes I, Nudel R, Iny Stein T, Levitt J, et al. MalaCards: an amalgamated
840   human disease compendium with diverse clinical and genetic annotation and structured search.
841   Nucleic Acids Res. 2017;45(D1):D877–87.
842 99. Alexa A, Rahnenfuhrer J. topGO: enrichment analysis for gene ontology. R package version.
843   2010;2(0):2010.
844 100. Vujovic D, Cornblath DR, Scherer SS. A recurrent MORC2 mutation causes Charcot-Marie-Tooth
845   disease type 2Z. Journal of the Peripheral Nervous System. 2021;26(2):184–6.
846 101. Sacoto MJG, Tchasovnikarova IA, Torti E, Forster C, Andrew EH, Anselm I, et al. De novo variants
847   in the ATPase module of MORC2 cause a neurodevelopmental disorder with growth retardation
848   and variable craniofacial dysmorphism. The American Journal of Human Genetics.
849   2020;107(2):352–63.
850 102. Lehti MS, Henriksson H, Rummukainen P, Wang F, Uusitalo-Kylmälä L, Kiviranta R, et al. Cilia-
851   related protein SPEF2 regulates osteoblast differentiation. Sci Rep. 2018;8(1):859.
852 103. Frankham R. Do island populations have less genetic variation than mainland populations?
853   Heredity (Edinb). 1997;78(3):311–27.
854 104. Frankham R. Effective population size/adult population size ratios in wildlife: a review. Genet Res
855   (Camb). 1995;66(2):95–107.
856 105. Morinha F, Dávila JA, Bastos E, Cabral JA, Frías Ó, González JL, et al. Extreme genetic structure in
857   a social bird species despite high dispersal capacity. Mol Ecol. 2017;26(10):2812–25.
858 106. Rising JD, Somers KM. The measurement of overall body size in birds. Auk. 1989;106(4):666–74.
859 107. Jolicoeur P. 193. Note: the multivariate generalization of the allometry equation. Biometrics.
860   1963;19(3):497–9.
861 108. Freeman S, Jackson WM. Univariate metrics are not adequate to measure avian body size. Auk.
862   1990;107(1):69–74.
863 109. Senar JC, Pascual J. Keel and tarsus length may provide a good predictor of avian body size.
864   ARDEA-WAGENINGEN-. 1997;85:269–74.
865 110. Grant PR, Grant BR. How and why species multiply: the radiation of Darwin's finches. Princeton
866   University Press; 2007.
867 111. Boag PT, Grant PR. Intense natural selection in a population of Darwin's finches (Geospizinae) in
868   the Galapagos. Science (1979). 1981;214(4516):82–5.
869 112. Gibbs HL, Grant PR. Oscillating selection on Darwin's finches. Nature. 1987;327(6122):511–3.
870 113. Tattersall GJ, Arnaout B, Symonds MRE. The evolution of the avian bill as a thermoregulatory
871   organ. Biological Reviews. 2017;92(3):1630–56.
872 114. Gamboa MP, Ghalambor CK, Scott Sillett T, Morrison SA, Chris Funk W. Adaptive divergence in
873   bill morphology and other thermoregulatory traits is facilitated by restricted gene flow in song
874   sparrows on the California Channel Islands. Mol Ecol. 2022;31(2):603–19.
875 115. Grant PR. EcologyandEvolutionofDarwin, sFinches · PrincetonUniversity Press. Princeton; 1986.
876 116. Price TD, Grant PR, Gibbs HL, Boag PT. Recurrent patterns of natural selection in a population of
877   Darwin's finches. Nature. 1984;309(5971):787–9.
878 117. Conway Morris S. Evolution: like any other science it is predictable. Philosophical Transactions of
879   the Royal Society B: Biological Sciences. 2010;365(1537):133–45.

880 118. Blount ZD, Lenski RE, Losos JB. Contingency and determinism in evolution: Replaying life's tape.
881   Science (1979). 2018;362(6415):eaam5979.
882 119. Charlesworth B. Measures of divergence between populations and the effect of forces that
883   reduce variability. Mol Biol Evol. 1998;15(5):538–43.
884 120. Burt DW. Origin and evolution of avian microchromosomes. Cytogenet Genome Res. 2002;96(1–
885   4):97–112.
886 121. Kaplan NL, Hudson RR, Langley CH. The" hitchhiking effect" revisited. Genetics. 1989;123(4):887–
887   99.
888 122. Dorsett D, Krantz ID. On the molecular etiology of Cornelia de Lange syndrome. Ann N Y Acad Sci.
889   2009;1151(1):22–37.
890 123. Bhuiyan Z, Klein M, Hammond P, mam Mannens M, Van Haeringen A, Van Berckelaer-Onnes I, et
891   al. Genotype-phenotype correlations of 39 patients with Cornelia De Lange syndrome: the Dutch
892   experience. J Med Genet. 2005;
893 124. Jackson L, Kline AD, Barr MA, Koch S De. de Lange syndrome: a clinical review of 310 individuals.
894   Am J Med Genet. 1993;47(7):940–6.
895 125. Faramarz A, Balk JA, Oostra AB, Ghandour CA, Rooimans MA, Wolthuis RMF, et al. Non-
896   Redundant Roles in Sister Chromatid Cohesion of the DNA Helicase DDX11 and the SMC3 Acetyl
897   Transferases ESCO1/2. bioRxiv. 2019;704635.
898 126. Alkhunaizi E, Shaheen R, Bharti SK, Joseph-George AM, Chong K, Abdel-Salam GMH, et al.
899   Warsaw breakage syndrome: Further clinical and genetic delineation. Am J Med Genet A.
900   2018;176(11):2404–18.
901 127. Ren S, Lyu G, Irwin DM, Liu X, Feng C, Luo R, et al. Pooled sequencing analysis of geese (Anser
902   cygnoides) reveals genomic variations associated with feather color. Front Genet.
903   2021;12:650013.
904 128. Domyan ET, Hardy J, Wright T, Frazer C, Daniels J, Kirkpatrick J, et al. SOX10 regulates multiple
905   genes to direct eumelanin versus pheomelanin production in domestic rock pigeon. Pigment Cell
906   Melanoma Res. 2019;32(5):634–42.
907 129. Bruders R, Van Hollebeke H, Osborne EJ, Kronenberg Z, Maclary E, Yandell M, et al. A copy
908   number variant is associated with a spectrum of pigmentation patterns in the rock pigeon
909   (Columba livia). PLoS Genet. 2020;16(5):e1008274.
910 130. Gazda MAnna. Genetic Basis of Simple and Complex Traits with Relevance to Avian Evolution.
911   [Porto]: Universidade do Porto ; 2019.
912 131. Bradley BJ, Gerald MS, Widdig A, Mundy NI. Coat color variation and pigmentation gene
913   expression in rhesus macaques (Macaca mulatta). J Mamm Evol. 2013;20:263–70.
914 132. Asogwa NC, Mori C, Sánchez-Valpuesta M, Hayase S, Wada K. Inter-and intra-specific differences
915   in muscarinic acetylcholine receptor expression in the neural pathways for vocal learning in
916   songbirds. Journal of Comparative Neurology. 2018;526(17):2856–69.
917 133. Qi LM, Mohr M, Wade J. Enhanced expression of tubulin-specific chaperone protein a,
918   mitochondrial ribosomal protein S27, and the DNA excision repair protein XPACCH in the song
919   system of juvenile male zebra finches. Dev Neurobiol. 2012;72(2):199–207.
920 134. Shi Z, Zhang Z, Schaffer L, Huang Z, Fu L, Head S, et al. Dynamic transcriptome landscape in the
921   song nucleus HVC between juvenile and adult zebra finches. Advanced Genetics.
922   2021;2(1):e10035.
923 135. Lovell P V, Clayton DF, Replogle KL, Mello C V. Birdsong "transcriptomics": neurochemical
924   specializations of the oscine song system. PLoS One. 2008;3(10):e3440.
925 136. Oikkonen J, Onkamo P, Järvelä I, Kanduri C. Convergent evidence for the molecular basis of
926   musical traits. Sci Rep. 2016;6(1):39707.

927 137. Yap CC, Winckler B. Harnessing the power of the endosome to regulate neural development.
928   Neuron. 2012;74(3):440–51.

929 138. Harris TJC, Tepass U. Adherens junctions: from molecules to morphogenesis. Nat Rev Mol Cell
930   Biol. 2010;11(7):502–14.

931 139. Delmore KE, Hübner S, Kane NC, Schuster R, Andrew RL, Câmara F, et al. Genomic analysis of a
932   migratory divide reveals candidate genes for migration and implicates selective sweeps in
933   generating islands of differentiation. Mol Ecol. 2015;24(8):1873–88.

934 140. Doxsey S, McCollum D, Theurkauf W. Centrosomes in cellular regulation. Annu Rev Cell Dev Biol.
935   2005;21:411–34.

936 141. Yeaman S. Genomic rearrangements and the evolution of clusters of locally adaptive loci.
937   Proceedings of the National Academy of Sciences. 2013;110(19):E1743–51.

938 142. Hoffmann AA, Sgrò CM, Weeks AR. Chromosomal inversion polymorphisms and adaptation.
939   Trends Ecol Evol. 2004;19(9):482–8.

940 143. Ayala D, Ullastres A, González J. Adaptation through chromosomal inversions in Anopheles. Front
941   Genet. 2014;5:129.

942 144. Christmas MJ, Wallberg A, Bunikis I, Olsson A, Wallerman O, Webster MT. Chromosomal
943   inversions associated with environmental adaptation in honeybees. Mol Ecol. 2019;28(6):1358–
944   74.

945 145. Feng W, Leach SM, Tipney H, Phang T, Geraci M, Spritz RA, et al. Spatial and temporal analysis of
946   gene expression during growth and fusion of the mouse facial prominences. PLoS One.
947   2009;4(12):e8066.

948 146. Campeau PM, Lenk GM, Lu JT, Bae Y, Burrage L, Turnpenny P, et al. Yunis-Varon syndrome is
949   caused by mutations in FIG4, encoding a phosphoinositide phosphatase. The American Journal of
950   Human Genetics. 2013;92(5):781–91.

951 147. Zinzow-Kramer WM, Horton BM, McKee CD, Michaud JM, Tharp GK, Thomas JW, et al. Genes
952   located in a chromosomal inversion are correlated with territorial song in white-throated
953   sparrows. Genes Brain Behav. 2015;14(8):641–54.

954 148. Law R, Dixon-Salazar T, Jerber J, Cai N, Abbasi AA, Zaki MS, et al. Biallelic truncating mutations in
955   FMN2, encoding the actin-regulatory protein Formin 2, cause nonsyndromic autosomal-recessive
956   intellectual disability. The American Journal of Human Genetics. 2014;95(6):721–8.

957 149. Gorukmez O, Gorukmez O, Ekici A. A novel nonsense FMN2 mutation in nonsyndromic autosomal
958   recessive intellectual disability syndrome. Fetal Pediatr Pathol. 2021;40(6):702–6.

959 150. Moloney GM, van Oeffelen WEPA, Ryan FJ, van de Wouw M, Cowan C, Claesson MJ, et al.
960   Differential gene expression in the mesocorticolimbic system of innately high-and low-impulsive
961   rats. Behavioural Brain Research. 2019;364:193–204.

962 151. Jaiswal SK, Gupta A, Shafer A, PK VP, Vijay N, Sharma VK. Genomic insights into the molecular
963   basis of sexual selection in birds. Front Ecol Evol. 2021;2.

964 152. De Luca F, Barnes KM, Uyeda JA, De-Levi S, Abad V, Palese T, et al. Regulation of growth plate
965   chondrogenesis by bone morphogenetic protein-2. Endocrinology. 2001;142(1):430–6.

966 153. Deng C, Wynshaw-Boris A, Zhou F, Kuo A, Leder P. Fibroblast growth factor receptor 3 is a
967   negative regulator of bone growth. Cell. 1996;84(6):911–21.

968 154. Yang Y, Topol L, Lee H, Wu J. Wnt5a and Wnt5b exhibit distinct activities in coordinating
969   chondrocyte proliferation and differentiation. 2003;

970 155. Abzhanov A, Protas M, Grant BR, Grant PR, Tabin CJ. Bmp4 and morphological variation of beaks
971   in Darwin's finches. Science (1979). 2004;305(5689):1462–5.

972 156. Brugmann SA, Powder KE, Young NM, Goodnough LH, Hahn SM, James AW, et al. Comparative
973   gene expression analysis of avian embryonic facial structures reveals new candidates for human
974   craniofacial disorders. Hum Mol Genet. 2010;19(5):920–30.

975 157. Enbody ED, Sendell-Price AT, Sprehn CG, Rubin CJ, Visscher PM, Grant BR, et al. Community-wide
976   genome sequencing reveals 30 years of Darwin's finch evolution. Science (1979).
977   2023;381(6665):eadf6218.
978 158. Pritchard JK, Di Rienzo A. Adaptation–not by sweeps alone. Nat Rev Genet. 2010;11(10):665–7.
979 159. Bosse M, Spurgin LG, Laine VN, Cole EF, Firth JA, Gienapp P, et al. Recent natural selection causes
980   adaptive evolution of an avian polygenic trait. Science (1979). 2017;358(6361):365–8.
981 160. Elmer KR, Fan S, Kusche H, Luise Spreitzer M, Kautt AF, Franchini P, et al. Parallel evolution of
982   Nicaraguan crater lake cichlid fishes via non-parallel routes. Nat Commun. 2014;5(1):5168.
983 161. Hoekstra HE, Hirschmann RJ, Bundey RA, Insel PA, Crossland JP. A single amino acid mutation
984   contributes to adaptive beach mouse color pattern. Science (1979). 2006;313(5783):101–4.
985 162. Steiner CC, Römpler H, Boettger LM, Schöneberg T, Hoekstra HE. The genetic basis of phenotypic
986   convergence in beach mice: similar pigment patterns but different genes. Mol Biol Evol.
987   2009;26(1):35–45.
988 163. Wittkopp PJ, Williams BL, Selegue JE, Carroll SB. Drosophila pigmentation evolution: divergent
989   genotypes underlying convergent phenotypes. Proceedings of the National Academy of Sciences.
990   2003;100(4):1808–13.
991 164. Monroe JG, Srikant T, Carbonell-Bejerano P, Becker C, Lensink M, Exposito-Alonso M, et al.
992   Mutation bias reflects natural selection in Arabidopsis thaliana. Nature. 2022;602(7895):101–5.
993 165. Liu X, Li YI, Pritchard JK. Trans effects on gene expression can drive omnigenic inheritance. Cell.
994   2019;177(4):1022–34.
995 166. Fagny M, Austerlitz F. Polygenic adaptation: integrating population genetics and gene regulatory
996   networks. Trends in Genetics. 2021;37(7):631–8.
997 167. Clements JF, Schulenberg TS, Iliff MJ, Roberson D, Fredericks TA, Sullivan BL, et al. The
998   eBird/Clements checklist of birds of the world: v2019. 2019.
999
1000

1001   **Tables**

1002
1003   **Table 1.** Divergence and diversity across the genome. Mean values, standard deviation and range of

1004   genomic summary statistics for the four species, including: Samples sizes for the continental and insular

1005   populations (N_{cont} and N_{is}), fixation Index (F_{ST}), absolute genomic divergence (d_{xy}), and genetic diversity
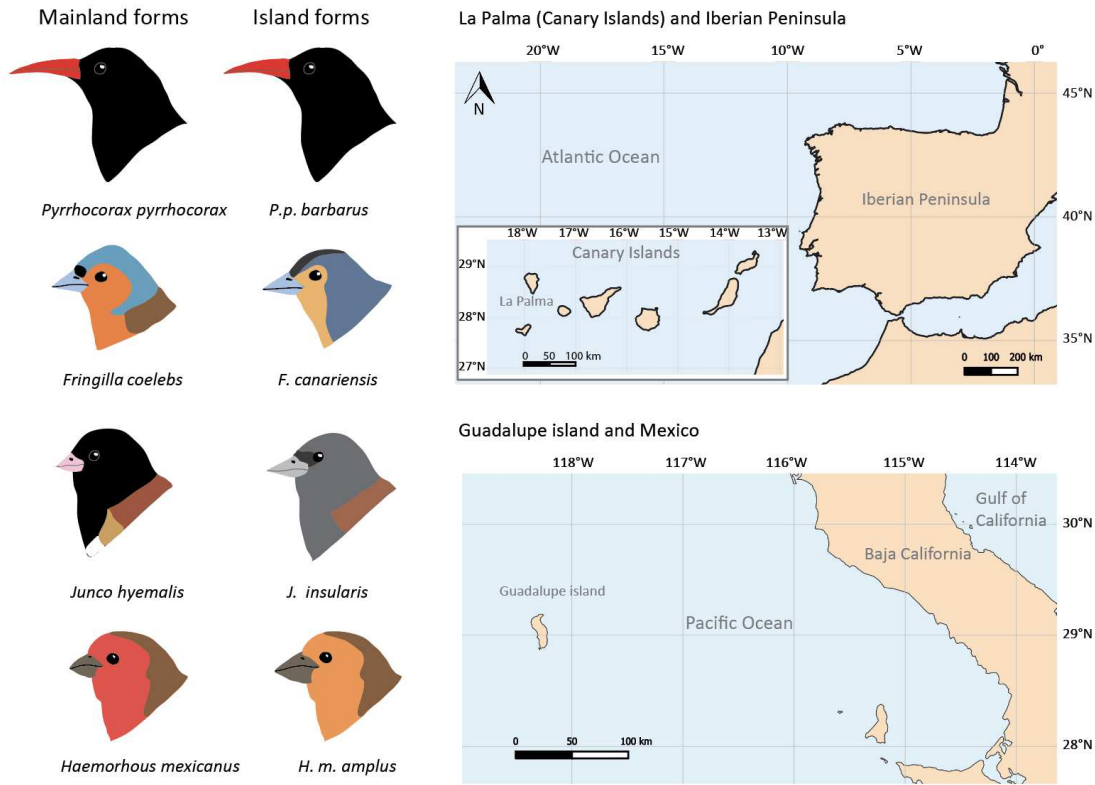
1006   for the insular and the continental populations.

Species	N_{cont}	N_{is}	F_{ST} ± sd	range	d_{xy} ± sd	range	π_{island} ± sd	range	$\pi_{continent}$ ± sd	range
Red-billed chough	12	12	0.21 ± 0.12	[-0.055 - 0.89]	0.0008 ± 0.0004	[0 - 0.15]	0.0005 ± 0.003	[0 - 0.013]	0.0008 ± 0.0004	[0 - 0.020]
House finch	12	12	0.14 ± 0.09	[-0.45 - 0.66]	0.006 ± 0.002	[0 - 0.017]	0.0043 ± 0.002	[0 - 0.018]	0.0052 ± 0.002	[0 - 0.016]
Dark-eyed junco	12	12	0.26 ± 0.07	[0.006 - 0.68]	0.005 ± 0.002	[0 - 0.023]	0.0022 ± 0.001	[0 - 0.023]	0.0049 ± 0.002	[0 - 0.022]
Common chaffinch	9	12	0.40 ± 0.05	[-0.033 - 0.88]	0.009 ± 0.003	[0 - 0.022]	0.0016 ± 0.001	[0 - 0.021]	0.0091 ± 0.003	[0 - 0.023]

1007
1008
1009

Figures

Mainland forms Island forms

Pyrrhocorax pyrrhocorax *P.p. barbarus*

Fringilla coelebs *F. canariensis*

Junco hyemalis *J. insularis*

Haemorhous mexicanus *H. m. amplus*

La Palma (Canary Islands) and Iberian Peninsula

Guadalupe island and Mexico

1011

1012 **Figure 1. Target taxa for comparative analysis.** (A) Species that have colonized La Palma in the Atlantic

1013 Ocean: the red-billed chough and the common chaffinch. (B) Species that have colonized Guadalupe

1014 island in the Pacific Ocean: the dark-eyed junco and the house finch. Bird species according to Clements

1015 et al., (167).

1016
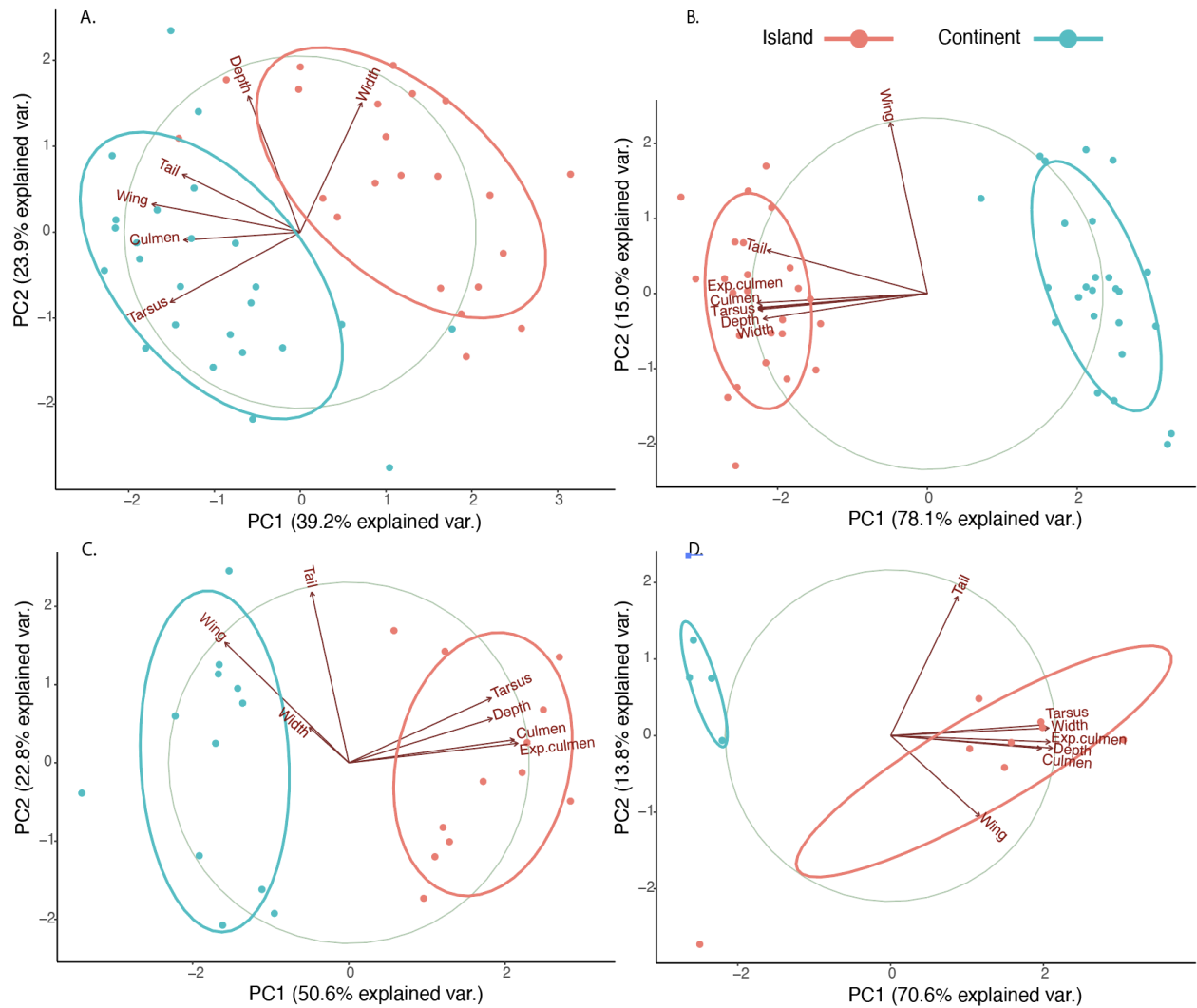
Figure 2. Principal Component Analysis (PCA) with morphological data per species A) Red-billed chough, B) Common/Canary Islands chaffinch, C) Dark-eyed/island junco, D) House finch. The variables included are wing, tail and tarsus length and bill depth, width, culmen and exposed culmen (the latter is not included for the red-billed chough). The correlation circle with radius 1 show the loadings of each variable that are represented by the arrows. The variables included are wing, tail and tarsus length and bill depth, width, culmen and exposed culmen (the latter is not included for the red-billed chough). Red and blue markers correspond to insular and mainland individuals, respectively.
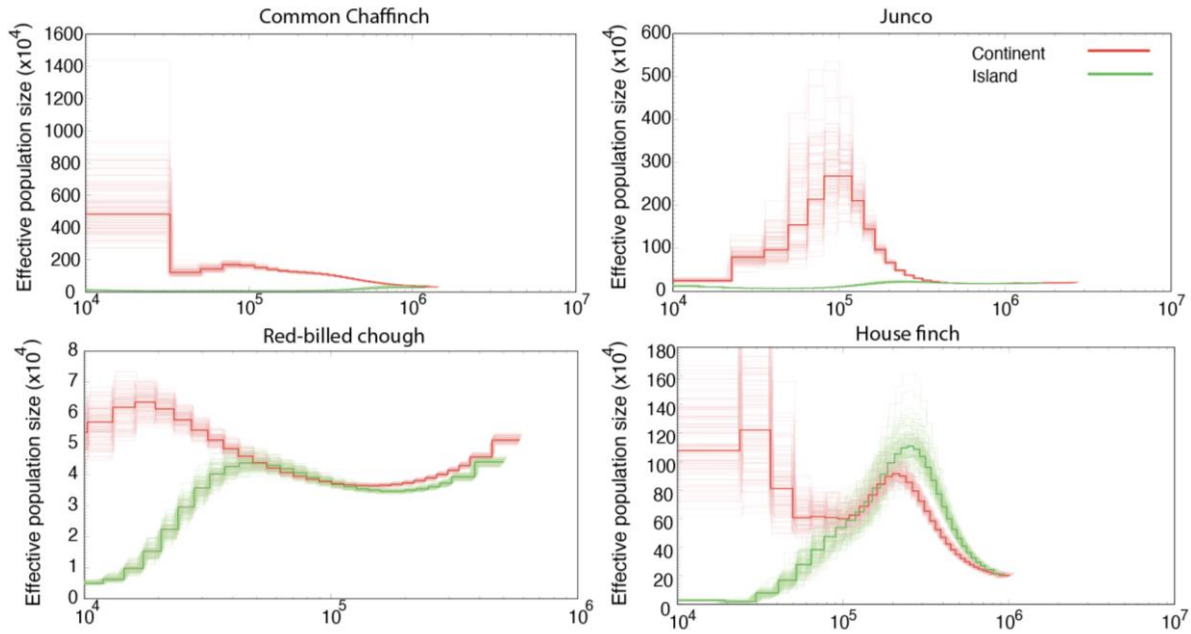
1028
1029   **Figure 3.** Demographic history of insular and mainland populations. The analysis was performed using

1030   Pairwise Sequentially Markovian Coalescent (PSMC). Demographic inference for one individual per

1031   treatment and species, with the red and green dark lines corresponding to the continental and insular

1032   populations, respectively. The lighter red and green lines represent 100 bootstrap replicates. The point

1033   where both lines depart from each other corresponds to the time of colonization, which is around

1034   40,000 y for the red-billed chough, 900,000 y for the common chaffinch, 100,000 y for the house finch

1035   and 400,000 y for the dark-eye junco. The mutation rate used was of 4.6e-9 mutation/site/generation

1036   for all species, and the generation time used in all cases was two years. See Fig. S2 for bootstrapped

1037   versions of the individual PSMC plots.

1038
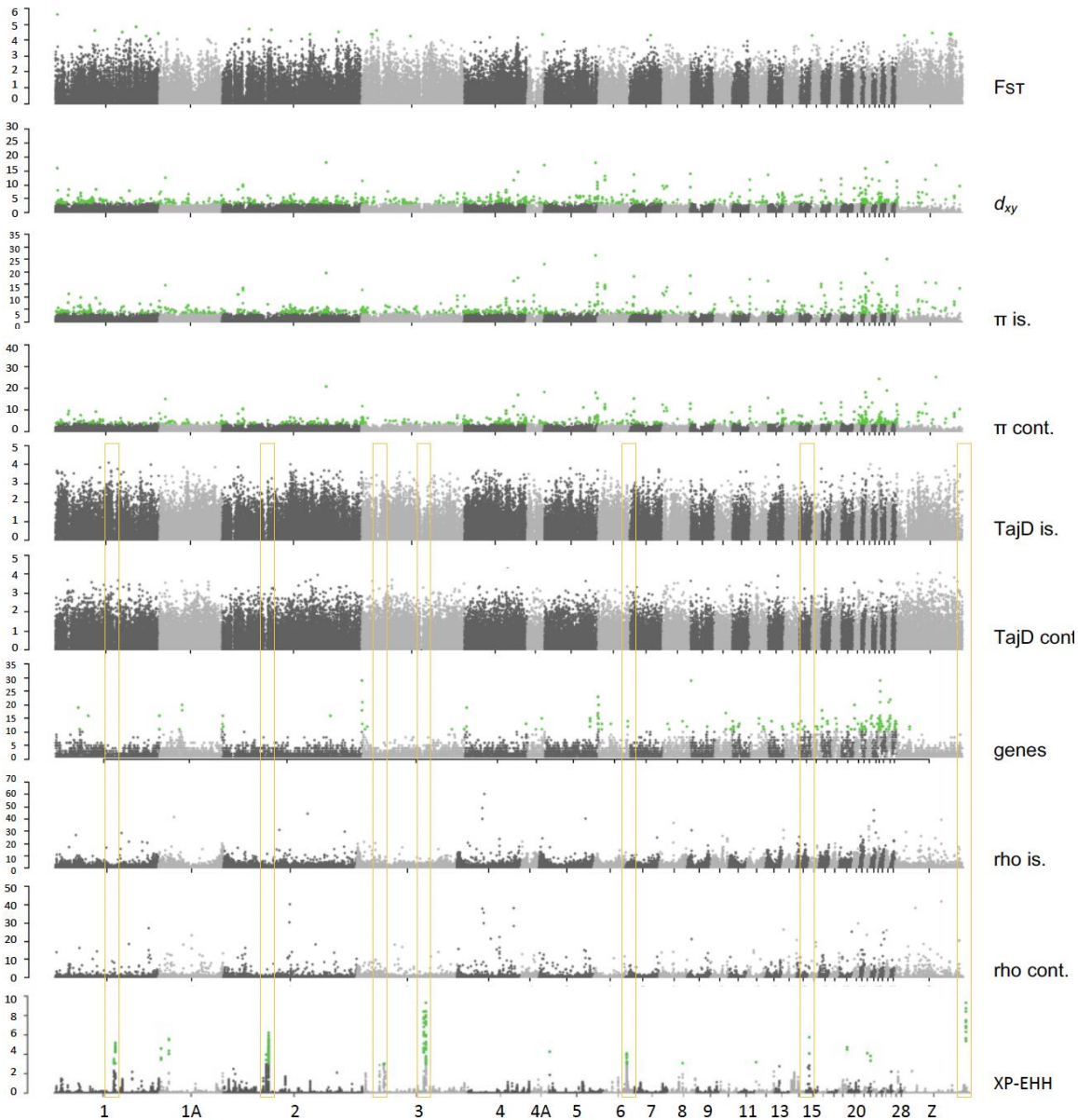
1039
1040 **Figure 4.** Genomic scans for several summary statistics for an island-mainland comparison in the red-

1041 billed chough (*Pyrrhocorax pyrrhocorax*). From top to bottom, fixation index (F_{ST}), genomic divergence

1042 (d_{xy}), genetic diversity for insular and continental populations (π), Tajima's D for insular and continental

1043 populations (TajD), number of genes, recombination rates for insular and mainland populations (rho)

1044 and Cross-populations Extended Haplotype Homozygosity (XP-EHH). Chromosome numbers correspond

1045 to the Zebra finch genome (*Taeniopygia guttata*). Green dots represent outliers with the false discovery

1046 rate (FDR) set at 0.05 after applying the Benjamini and Hochberg correction, except for the XP-EHH,

1047 where the threshold is set at $-\log_{10}$ (*p*-value) ≥ 3. The yellow boxes highlight the XP-EHH peaks

1048 coincident with drops in Tajima's D.
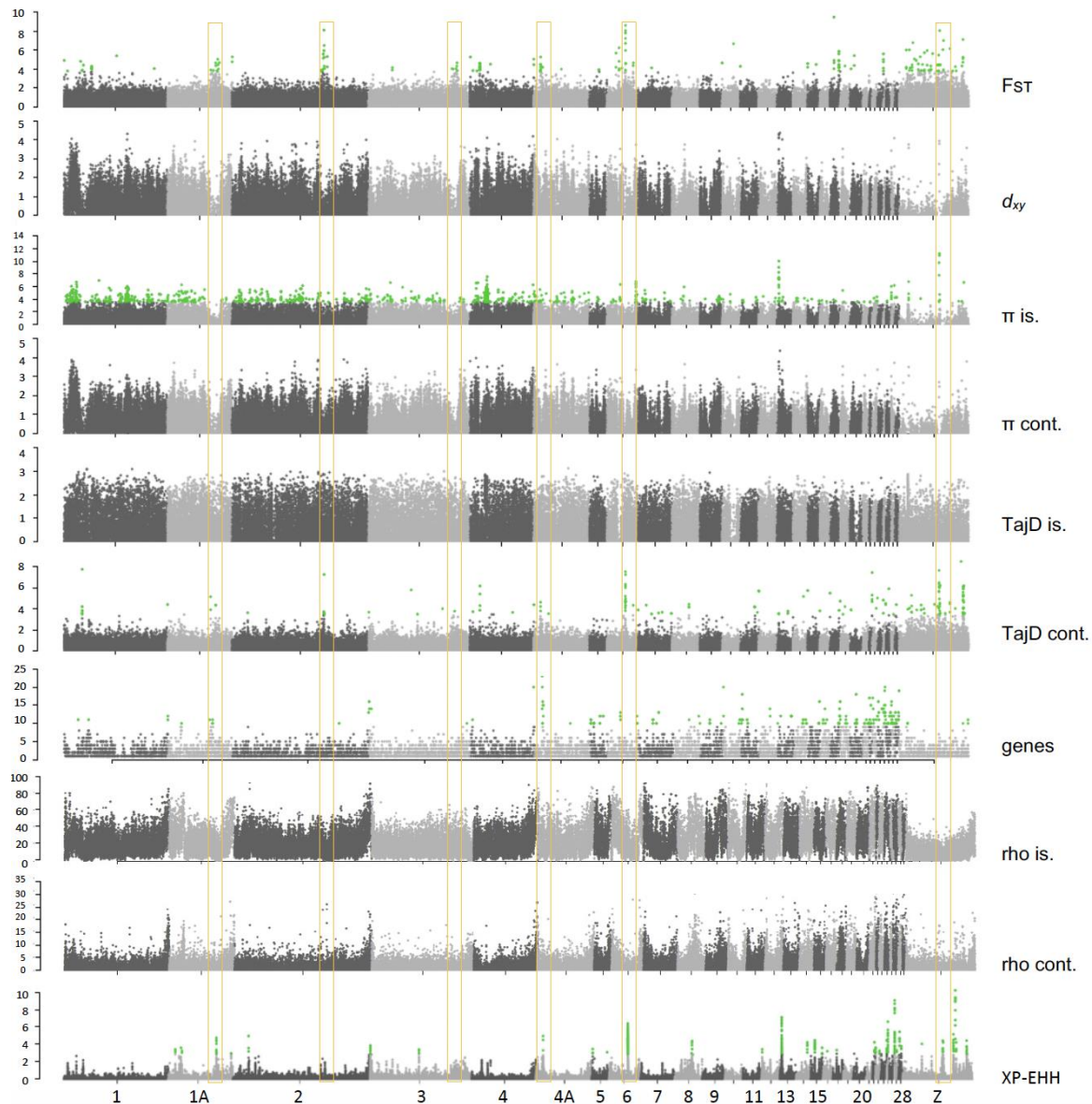
Figure 5. Genomic scans for several summary statistics for an island-mainland comparison in the common chaffinch (*Fringilla coelebs*). From top to bottom, fixation index (F_{ST}), genomic divergence (d_{xy}), genetic diversity for insular and continental populations (π), Tajima's D for insular and continental populations (TajD), number of genes, recombination rates for insular and mainland populations (rho) and Cross-populations Extended Haplotype Homozygosity (XP-EHH). Chromosome numbers correspond to the Zebra finch genome (*Taeniopygia guttata*). Green dots represent outliers with the false discovery rate (FDR) set at 0.05 after applying the Benjamini and Hochberg correction, except for the XP-EHH, where the threshold is set at $-\log_{10}$ (*p*-value) ≥ 3. The yellow boxes highlight the signatures of recurrent selection (F_{ST} peaks coincident with drops in d_{xy} and π). Some of them are also coincident with peaks in XP-EHH.
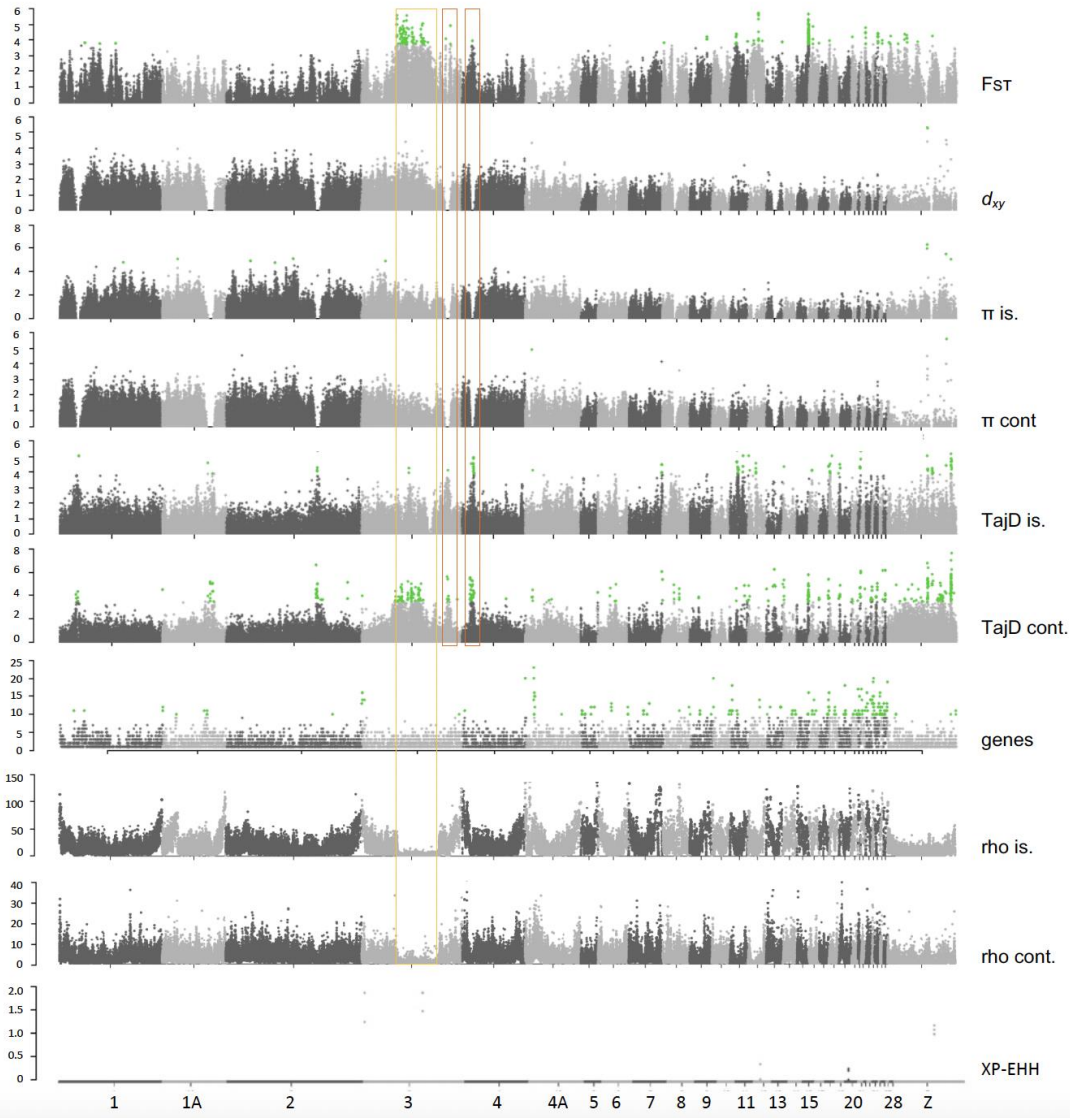
1060
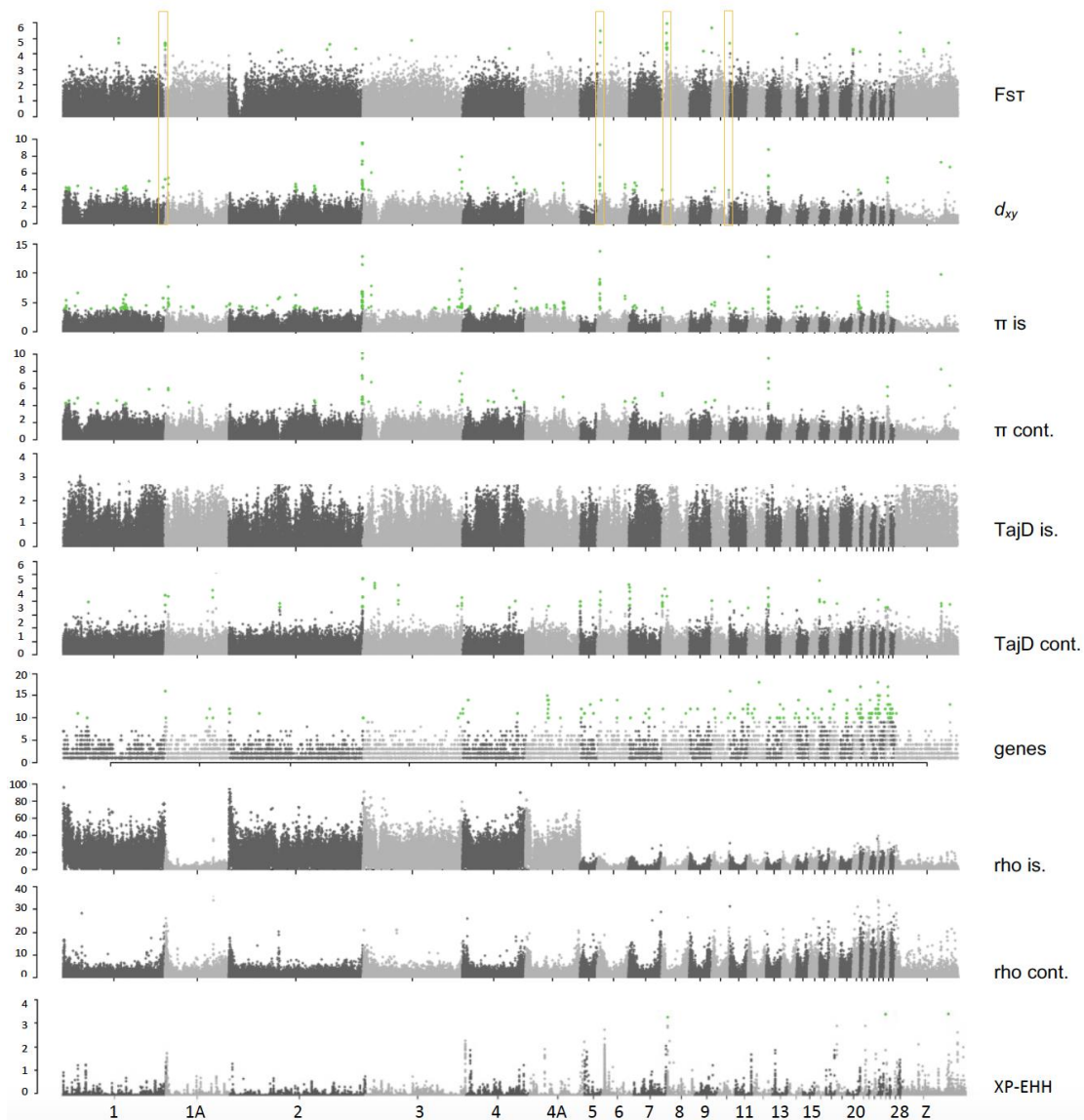
1061
1062 **Figure 6.** Genomic scans for several summary statistics for an island-mainland comparison in the dark-

1063 eyed junco (*Junco hyemalis*). From top to bottom, fixation index (F_{ST}), genomic divergence (d_{xy}),

1064 genetic diversity for insular and continental populations (π), Tajima's D for insular and continental populations

1065 (TajD), number of genes, recombination rates por insular and mainland populations (rho) and Cross-

1066 populations Extended Haplotype Homozygosity (XP-EHH). Chromosome numbers correspond to the

1067 Zebra finch genome (*Taeniopygia guttata*). Green dots represent outliers with the false discovery rate

1068 (FDR) set at 0.05 after applying the Benjamini and Hochberg correction, except for the XP-EHH, where

1069 the threshold is set at −log10 (*p*-value) ≥ 3. The yellow boxes highlight the F_{ST} peaks in the chromosome

1070 extremes.

1071

1072

Figure 7. Genomic scans for several summary statistics for an island-mainland comparison in the house
finch (*Haemorhous mexicanus*). From top to bottom, fixation index (F_{ST}), genomic divergence (d_{xy}),
genetic diversity for insular and continental populations (π), Tajima's D for insular and continental
populations (TajD), number of genes, recombination rates por insular and mainland populations (rho)
and Cross-populations Extended Haplotype Homozygosity (XP-EHH). Chromosome numbers correspond
to the Zebra finch genome (*Taeniopygia guttata*). Green dots represent outliers with the false discovery
rate (FDR) set at 0.05 after applying the Benjamini and Hochberg correction, except for the XP-EHH,
where the threshold is set at $-\log10$ (*p*-value) ≥ 3. The yellow box highlights the putative inversion in
chromosome 3 (F_{ST} peak that coincides with a drop in the recombination rate). The orange boxes
highlight the signatures of recurrent selection (F_{ST} peak coincident with drops in d_{xy} and π).

Supplementary Files

This is a list of supplementary files associated with this preprint. Click to download.

- RecuerdaetalBMCSupplementaryMaterials.docx